Hunting for Pirated Software Using Metamorphic Analysis

Hardikkumar Rana
San Jose State University

Hunting for Pirated Software Using Metamorphic Analysis

A Project

Presented to

The Faculty of the Department of Computer Science

San Jose State University

In Partial Fulfillment

of the Requirements for the Degree

Master of Science

by

Hardikkumar Rana

May 2014

The Designated Project Committee Approves the Project Titled

Hunting for Pirated Software Using Metamorphic Analysis

by

Hardikkumar Rana

APPROVED FOR THE DEPARTMENTS OF COMPUTER SCIENCE

SAN JOSE STATE UNIVERSITY

May 2014

Dr. Mark Stamp	Department of Computer Science
Dr. Chris Pollett	Department of Computer Science
Dr. Thomas Austin	Department of Computer Science

ABSTRACT

Hunting for Pirated Software Using Metamorphic Analysis

by Hardikkumar Rana

In this paper, we consider the problem of detecting software that has been pirated and modified. We analyze a variety of detection techniques that have been previously studied in the context of malware detection. For each technique, we empirically determine the detection rate as a function of the degree of modification of the original code. We show that the code must be greatly modified before we fail to reliably distinguish it, and we show that our results offer a significant improvement over previous related work. Our approach can be applied retroactively to any existing software and hence, it is both practical and effective.

ACKNOWLEDGMENTS

I would like to thank my advisor Dr. Mark Stamp for his continuous guidance and support throughout this project and believing in me. I would also like to thank him for giving me a chance to work on this topic. I would like to thank the committee members Dr. Chris Pollett and Dr. Thomas Austin for monitoring the progress of the project, their feedback and advice. Last but not least, I would like to thank my parents and sister for their love and support.

TABLE OF CONTENTS

LIST OF TABLES

LIST OF FIGURES

CHAPTER 1

Introduction

Software piracy can be defined as the unauthorized reproduction of software, distribution of copyrighted software including downloading, sharing, selling, or installing multiple copies of licensed software [30, 33]. The Business Software Alliance (BSA) is a major anti-piracy organization. According to a 2010 BSA study, the commercial value of pirated software increased 14% globally in 2010 to a record total of $58.8 billion [31]. They estimate that almost 41% of all software installed on personal computers is pirated, and for every dollar of software sale, $3 to $4 revenue is lost to local IT support and distribution service [32]. Thus, software piracy drains significant revenue that might otherwise have been spent on salaries and innovation.

Pirated software is also a threat to security [32]. To defend against attacks, software developers release fixes and patches. Software users who use pirated or unlicensed copies of software are unable to benefit from patches and important updates, which may decrease their security, as well as the security of other licensed users [32].

The goal of this research is to develop techniques that help to detect modified pirated software. Detection of unmodified software is comparatively a trivial problem. An attacker might modify software as a way to obtain the functionality, while trying to maintain an air of legitimacy and also avoid copyright infringement issues [24]. Ideally, we would like to force the attacker to make major changes to the software before we cannot reliably detect it.

The techniques developed here are designed to be used as an automated first line of analysis. For example, if a company suspects their software has been illegally copied and modified, they can compare the suspected variant to the original using the techniques in this paper. A high score indicates that further (costly) investigation is warranted, whereas a low score indicates that the suspect code differs significantly from the original code, and hence, further analysis would be a waste of resources.

Here, we consider a variety of techniques, and for all techniques, we require access to executable files only—no source code is used in the analysis. This is important, because we are unlikely to have the source code of the suspect software. Some of our techniques rely on assembly code, which can be extracted via disassembly, whereas others apply directly to the executable.

For all of the techniques considered in this report, no special effort is required at the time the software is developed and hence, the analysis presented here can be applied retroactively to any executable. Consequently, the research in this paper should not be confused with watermarking schemes, which require that a mark be embedded in the executable. Although our approach has some superficial similarity to software plagiarism detection, we suspect it may not be strong in such a scenario. We analyze the software from a low level perspective with the emphasis on structural and statistical properties, whereas plagiarism detection is generally focused on higher-level semantics and stylistic issues [7, 17, 28].

The techniques we consider fit loosely in the realm of software birthmark analysis [22, 39]. A software birthmark is a unique characteristic inherent to the software, which can be used for identification. All the techniques we proposed in the paper were previously used for metamorphic malware detection. We used these techniques for completely different approach of software piracy detection. Some previous work on the software piracy detection relied on statistical analysis, whereas, we used some novel approaches based on compression based analysis and singular value decomposition. For all the techniques, neither the original nor the suspected software are executed. The results of our experiment indicate that software must be modified extensively to make it undetectable.

The techniques we analyze in this paper were inspired by previous research on metamorphic virus detection [13, 16, 26, 27, 44]. Metamorphic malware changes its internal structure at each infection, while maintaining its essential function. Such malware can easily evade signature-based detection and well-designed metamorphic malware can also evade statistical-based detection. Malware detection provides some parallels to the problem considered here, but there are also significant differences. These similarities and differences will become clear in subsequent sections.

The remainder of this paper is organized as follow. Chapter 2 discusses background material on metamorphic malware (software), metamorphic generator and metamorphism techniques. Also, it covers background information about all the proposed techniques: hidden Markov model, opcode graph similarity, simple substitution distance, singular value decomposition, and compression-based analysis. In Chapter 3, we provide details on implementation. Experimental results and observation are explained in Chapter 4. Finally, Chapter 5 contains conclusions and future work.

CHAPTER 2

Background

In this chapter, we will discuss background information required to understand the project. Starting with metamorphic malware (software), then metamorphic generator and morphing techniques. After that we will cover background information about all the proposed techniques named Hidden Markov Model, Opcode Graph Similarity, Simple Substitution Distance, Singular Value Decomposition, and Compression Based Analysis.

2.1 Metamorphic Malware/Software

Metamorphic malware changes its internal structure after each infection, but its functionality remains the same. This technique is used by malware writers to evade anti-virus [38].

Metamorphism has some positive sides too. It can be used to raise diversity for the given software [36]. One can derive an interesting analogy between software and the biological system [37]. Large amount of the population survives in case of attack on biological system [37] due to diversity among the population. However, as software can be seen as a monoculture [37], a successful attack on one software works almost on every other software [37]. In the case of metamorphic software, no single attack will be successful on every copy of the software [37].

2.2 Metamorphic Generator

A metamorphic generator can be implemented in any language using different morphing techniques. We will discuss these techniques in the following section. We

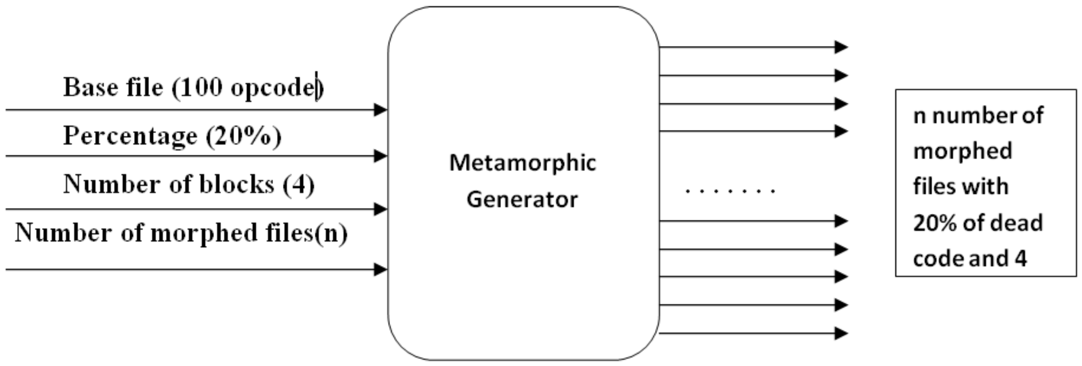

Figure 1: Metamorphic Generator

have chosen the dead code insertion technique for morphing. Ideally, the control and data flow of the code need to remain the same, and various jump statements can be used to achieve it. But, it would be easier to detect virus because of many jump statements. So, we did not try to maintain code execution sequence in same manner for morphed files, which eventually make harder case.

Initially, the program asks for morphing percentage and the number of blocks for dead code insertion. Suppose, that morphing percentage and number of blocks are given as 20 and 4 respectively, and we have a base file of 100 opcode. Then, the total number of opcode needed for dead code will be 20 and distributed 5 opcodes per block. Next, using random function of JAVA, it generates 4 random numbers for the position of dead code insertion. The output file will become the size of 120 opcode. We can generate as many morphed files as required using metamorphic generator. Morphing percentage is one of the measures to check the robustness of our detection techniques. Here, we are simulating the way an attacker could have targeted any piece of software using dead code insertion.

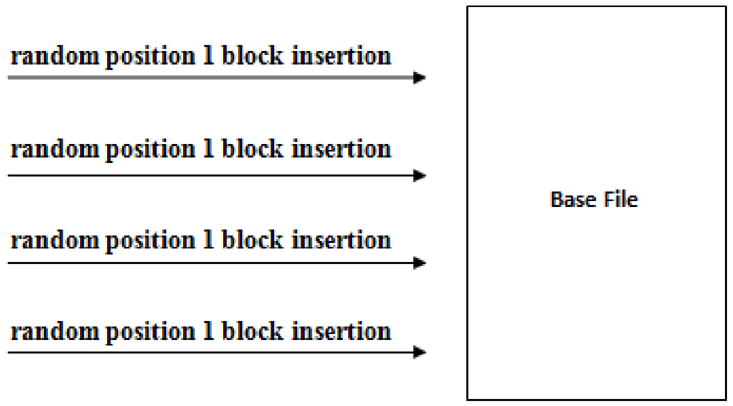
random position 1 block insertion
random position 1 block insertion
random position 1 block insertion
random position 1 block insertion
Base File

Figure 2: Block Insertion

2.3 Techniques for Metamorphism

In the following section, we discuss some common techniques to generate the metamorphic code like dead code insertion, code permutation, insertion of jump instruction, and instruction replacement.

2.3.1 Dead Code Insertion

Dead code insertion is one of the simplest methods of morphing used by a metamorphic engine. In this method, a sequence of bytes is changed by inserting the dead code [23]. Ideally, instructions used for the dead code should not have any effect on the functionality of the original code [15]. Dead code is similar to a null operation [14]. The inserted dead code will never be executed, so it has no semantic effect on the software [4]. This strategy could be used to evade signature based detection and is succeeding against statistical based detection [3]. The example shown in Table 1, demonstrates the dead code insertion.

Table 1: Dead Code Insertion

Original Code	After Garbage Insertion
`ADD 1055h, EAX`	`ADD 1055h, EAX`
`SUB EAX`	`JMP loc1234`
	`POP EBX`
	`PUSH EBX`
	`PUSH EBX`
	`POP EBX`
	`loc1234 SUB EAX`

In Table 1 we can see that, in the original code, execution of the `ADD` instruction is followed by `SUB`, whereas in the code after garbage insertion, `ADD` is followed by the `JMP`, which immediately transfers the control to the `SUB`. All the dead code between `ADD` and `SUB` is eliminated by `JMP` instruction and the dead code does not have any effect on the actual code execution.

2.3.2 Code Permutation

In this method, code is divided into small modules (frames). After dividing the code, different modules are rearranged randomly by keeping the logic of the original code as it is. Various jump statements are used to maintain the logic of the code. Figure 3 illustrates the code permutation technique. So, this technique apparently changes the appearance of the software by reordering the frame sequences. If we have n frames of the software, then $n!$ unique generations are possible [5].

2.3.3 Insertion of Jump Instructions

`JMP` is assembly language instruction. It carries out an unconditional jump. It takes memory address, which are labeled in assembly language, as arguments [23].

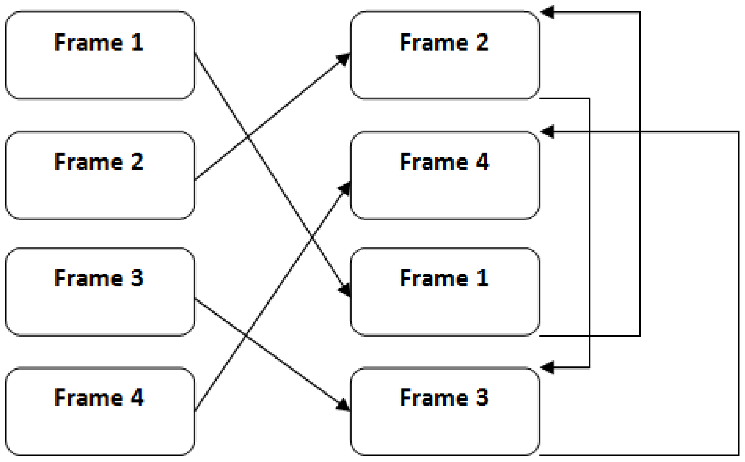

Figure 3: Code Permutation

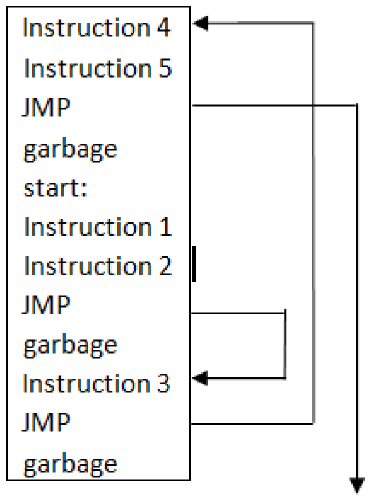

Figure 4: Insertion of Jump Instructions

`JMP` is used to change the address of targeted instruction. However, the flow of the program remains the same [23]. Many `JMP` are more prone to detections as it provides the identification.

2.3.4 Instruction Replacement

In this method, instruction or a set of instructions is replaced by equivalent instruction or set of instructions. For example, different registers movements are

Table 2: Instruction Replacement

Original Code	After Instruction Replacement
`ADD EAX, 05H`	`ADD EAX, 01H`
`MOV BL, AL`	`ADD EAX, 05H`
	`PUSH BL`
	`POP AL`

replaced by number of `PUSH` and `POP` sequences. Instructions like `OR-TEST` and `XOR-SUB` can be used interchangeably [15]. Table 2 illustrates the instruction replacement techniques. Here, in the code after instruction replacement, `ADD` is replaced with two `ADD` instructions and `MOV` operation is performed using `PUSH` and `POP` operation. This technique defends strongly against the signature base detection.

2.4 Hidden Markov Model

A hidden Markov model (HMM) is a machine learning techniques [35]. As the name suggests, an HMM includes a Markov process and this process is the "hidden" part of the HMM. That is, the Markov process is not directly observable. But we do have indirect information about the Markov process via a series of observations that are probabilistically related to the underlying Markov process. The utility of HMMs derives largely from the fact that there are efficient algorithms for training and scoring. HMM have been used in various fields like malware detection [19] and speech recognition [25]. Following are the important notation to understand the Hidden Markov Model [35]:

$$
\begin{aligned}
T &= \text{length of the observation sequence}\\
N &= \text{number of states in the model}\\
M &= \text{number of observation symbols}\\
Q &= \{q_0, q_1, \ldots, q_{N-1}\} = \text{distinct states of the Markov process}\\
V &= \{0, 1, \ldots, M-1\} = \text{set of possible observations}\\
A &= \text{state transition probabilities}\\
B &= \text{observation probability matrix}\\
\pi &= \text{initial state distribution}\\
\mathcal{O} &= (\mathcal{O}_0, \mathcal{O}_1, \ldots, \mathcal{O}_{T-1}) = \text{observation sequence.}
\end{aligned}
$$

$$\begin{tikzcd}
\text{Markov process:} & X_0 \arrow[r, "A"] \arrow[d, "B"'] & X_1 \arrow[r, "A"] \arrow[d, "B"'] & X_2 \arrow[r, "A"] \arrow[d, "B"'] & \cdots \arrow[r, "A"] & X_{T-1} \arrow[d, "B"'] \\
\text{Observations:} & \mathcal{O}_0 & \mathcal{O}_1 & \mathcal{O}_2 & \cdots & \mathcal{O}_{T-1}
\end{tikzcd}$$

Figure 5: Hidden Markov Model

Three matrices A, B and π are used to define hidden Markov model. HMM is presented as $\lambda = (A, B, \pi)$. There are three basic problems that can be answered using hidden Markov model.

Problem 1: For a given model $\lambda = (A, B, \pi)$ and a sequence of observations $\mathcal{O}$, we can determine $P(O|\lambda)$. That is, we can score an observation sequence to determine how well it fits a given model [35].

Problem 2: For a given model $\lambda = (A, B, \pi)$ and a sequence of observations $\mathcal{O}$, we can determine an optimal state sequence for the Markov model. That is, we can uncover the hidden part of the model [35].

Problem 3: For a given observation sequence $\mathcal{O}$, and specific values of N and M we can determine a model. That is, we can train a model to fit a given observation sequence [35].

There are two main phases in HMM—Training and Detection. Training phase is to retrieve model that contains A, B, and π matrices. This model will be used for scoring files.

2.4.1 Training

In this phase, the opcode sequences are extracted from the base software. Using these opcode sequences, various slightly morphed copies of the base software are generated. These morphed copies are appended and finally hidden Markov model is trained on it. The reason for using slightly morphed copies is to avoid over fitting the training data for HMM [21]. At the end of the training phase, we retrieve A, B, and π.

2.4.2 Detection

In this phase, the opcode sequence from the suspected software is extracted. This sequence is scored against the trained HMM, which was derived in the previous phase. Then, score is compared against the previously calculated threshold value. The score above threshold indicates that further investigation is needed because suspected software is very similar to the base software. On the other hand, score below the threshold signifies that suspected software is not similar to the base software. In our case, we mainly interested in separation between benign files and suspected files. Therefore, we did not bother about setting the threshold.

2.5 Opcode Graph Similarity

The paper [1] suggests one interesting graph based technique for malware detection. The same technique can be used for the software similarity detection. Firstly, opcode sequence from the software is extracted to construct weighted directed graph. Each distinct opcode are assigned to the node in weighted directed graph. A directed edge is linked from a node to all the possible successor node. Weight of a particular edge gives the probability of corresponding successor node. The following example demonstrates the process. We used one dummy sequence of the opcodes as shown in the Table 3.

Using the Table 3, we obtained the counts for each digram of opcodes. These counts are shown in the Table 4. For example, the opcode `SUB` is immediately followed by the opcode `JMP` at 2 places (lines 10 and 20 in Table 3).

Using the digram frequency counts from Table 4, probability Table 5 is generated. Each cell in Table 5 represents a probability for occurrence of the given opcode after any opcode. Each entry in the Table 4 is divided by the sum of each entry of the corresponding row. The resulting probability table is shown in the Table 5. For example, `JMP` occurs 6 times in the table while (`JMP`, `SUB`) occurs 2 times. Therefore, (`JMP`, `SUB`) entry in the Table 5 contains the probability 1/3.

Using the entries from the Table 5 opcode directed graph is prepared. This directed probability graph is represented as adjacency matrix for ease of calculations.

Table 3: Opcode Sequence

1	CALL
2	JMP
3	ADD
4	SUB
5	NOP
6	CALL
7	ADD
8	JMP
9	JMP
10	SUB
11	JMP
12	ADD
13	NOP
14	JMP
15	CALL
16	CALL
17	CALL
18	ADD
19	JMP
20	SUB

Table 4: Opcode Count

	ADD	CALL	JMP	NOP	SUB
ADD	0	0	2	1	1
CALL	2	2	1	0	0
JMP	2	1	1	0	2
NOP	0	1	1	0	0
SUB	0	0	1	1	0

Table 5: Probability Table

	ADD	CALL	JMP	NOP	SUB
ADD	0/4	0/4	1/2	1/4	1/4
CALL	2/5	2/5	1/5	0/5	0/5
JMP	1/3	1/3	1/3	0/6	1/3
NOP	0/2	1/2	1/2	0/2	0/2
SUB	0/2	0/2	1/2	1/2	0/2

2.6 Simple Substitution Distance

Substitution cipher is one of the oldest cipher systems [36]. In this system, each plaintext symbol is substituted by ciphertext symbol. These symbols could be letters, digrams, or trigrams. There are many types of substitution ciphers. In the following section, we briefly discuss simple substitution ciphers.

2.6.1 Simple Substitution Ciphers

Simple Substitution ciphers are one of the simplest form of substitution ciphers [36]. In this cipher, plaintext symbol maps to one ciphertext symbol [9, 18]. A simple substitution key is shown in Table 6. In that, each ciphertext letter is obtained by shifting the plaintext letter by 3 positions forward in the alphabetical order [36]. Hence, plaintext message `HELLO` is encrypted to `KHOOR`, if the key in Table 6 is used for encryption [3].

Table 6: Simple Substitution Key

plaintext:	A	B	C	D	E	F	G	H	I	J	K	L	M	N	O	P	Q	R	S	T	U	V	W	X	Y	Z
ciphertext:	D	E	F	G	H	I	J	K	L	M	N	O	P	Q	R	S	T	U	V	W	X	Y	Z	A	B	C

Simple substitution consists 26! possible keys if plaintext is in the English language. To break the system attacker needs to try 2^{87} keys on average [9]. If the attacker has high computation power that can test 2^{40} keys per second, then brute force attack will take around 2^{47} seconds (millions of years) [9]. It is impractical to try such a huge key space. But attacker uses different approaches like English monograph statistic to crack the ciphertext [9]. For example, most frequent ciphertext letter maps to most frequent letter in the English text `E`, similarly second most frequent letter maps to second most frequent letter in the English text `T`, and so on. Using this technique, an attacker will be able to recover most of the plaintext very fast. Then, he can guess for the remaining message [9].

2.6.2 Fast Attack on Simple Substitution

An algorithm to crack the simple substitution cipher is mentioned in [12]. It initially guesses the key and modifies the key in each iteration by swapping elements in key. Correctness of key is determined by checking the closeness between digram matrix obtained from English plain text and decrypted text. The lower the score, the higher the correctness of the key. This algorithm is explained in section 2.6.4.

2.6.3 Solution Using Hill Climbing Problem

Hill climb is a mathematical optimized technique that starts with some initial solution and try to finds better solutions by doing minor changes to the putative solution. The new score is compared against the previous score. If the score improves, the incremental changes are made [9]. This process is repeated until the better solution is obtained [9, 43].

2.6.4 Overview of Jackobsen's Algorithm

Jackobsen's algorithm [12] make assumptions about plaintext and ciphertext. It assumes that plaintext and ciphertext are in English and contains 26 alphabets. It makes an initial guess about key using frequency of letters that is most frequent letter in ciphertext maps to the most frequent letter in English text `E`, second most frequent letter maps to `T`, and so on.

In the subsequent iterations, algorithm modifies the current key and uses it to decrypt ciphertext. If putative plaintext is closer to the expected English text than before, the new key is used for next iterations; otherwise the old key is modified in a different way. This process is repeated around $\binom{26}{2}$ times, so that every elements of key are swapped at least once.

The scheme to modify the key is explained in [9]. Suppose that the putative key is $K = k_1, k_2, k_3, k_4, \ldots, k_{25}, k_{26}$. Here, K is permutation of english letters. At beginning, the swapping takes place between adjacent elements. That is k_1 with k_2, k_2 with k_3 and so on. In the second iteration, elements away by two from each other are swapped, that is k_1 with k_3, k_2 with k_4 and so on. Same way in third iteration, elements away by three from each other are swapped. In the n^{th} iteration, elements away by n from each other are swapped. The process is presented diagrammatically in [9] which is shown in (1).

$$\begin{array}{ll}
\text{round 1:} & k_1|k_2 \;\; k_2|k_3 \;\; k_3|k_4 \;\; \ldots \;\; k_{23}|k_{24} \;\; k_{24}|k_{25} \;\; k_{25}|k_{26} \\
\text{round 2:} & k_1|k_3 \;\; k_2|k_4 \;\; k_3|k_5 \;\; \ldots \;\; k_{23}|k_{25} \;\; k_{24}|k_{26} \\
\text{round 3:} & k_1|k_4 \;\; k_2|k_5 \;\; k_3|k_6 \;\; \ldots \;\; k_{23}|k_{26} \\
\quad\vdots & \quad\vdots \qquad\qquad\quad \iddots \\
\text{round 24:} & k_1|k_{24} \;\; k_2|k_{25} \;\; k_3|k_{26} \\
\text{round 25:} & k_1|k_{25} \;\; k_2|k_{26} \\
\text{round 26:} & k_1|k_{26}
\end{array} \tag{1}$$

where, '|' means swap.

Using diagraph distribution matrix of putative key, the current key is modified [9]. This procedure is explained later in this section. To determine the closeness between digraph distribution matrix of putative plaintext and English language, the following scoring function (2) is used [9].

$$\text{score}(K) = d(D, E) = \sum_{i,j} |d_{i,j} - e_{i,j}| \tag{2}$$

Table 7: Frequency Count

E	T	A	O	I	N	S	R	H	D
11	9	5	4	4	6	3	5	2	12

Table 8: Putative Key K

Plaintext:	E	T	A	O	I	N	S	R	H	D
Ciphertext:	D	E	T	N	A	R	I	O	S	H

Where,

$D = d_{ij}$ represents the putative plaintext digraph distribution matrix

$E = e_{ij}$ represents the expected English language digraph distribution matrix

$K =$ similarity between two matrices (K is always greater than or equal to zero)

Procedure for modifying K is explained in [9]. We also mentioned it below. If we have simple substitution cipher that is based on English letters, descending order of plaintext symbols according to the frequency is

```
E, T, A, O, I, N, S, R, H, D
M, O, P, S, J, R, U, Y, B, K
```

Suppose the ciphertext is [27]

```
TNDEODRHISOADDRTEDOAHENSINEOARDTTDTINDDRNEDNTTTDDISRETEEEEEAA
```

The frequency count corresponding to the ciphertext is shown in Table 7 and the initial putative key K is shown in Table 8. Putative plaintext will be [9]

```
AOETRENDSHRIEENATERIDTOHSOTRINEAAEASOEENOTEOAAAEESHNTATTTTTII
```

Table 9: Diagraph Distribution Matrix

	E	T	A	O	I	N	S	R	H	D
E	3	1	2	1	0	3	1	1	0	0
T	2	4	1	1	1	0	0	2	0	0
A	2	2	2	1	0	0	1	0	0	0
O	2	2	1	0	0	0	0	0	1	0
I	1	0	0	0	1	1	0	0	0	1
N	1	1	1	1	0	0	0	0	0	1
S	0	0	0	2	0	0	0	0	2	0
R	1	0	0	0	3	0	0	0	0	0
H	0	0	0	0	0	1	1	1	0	0
D	0	1	0	0	0	0	1	0	0	0

Table 10: New Putative Key

Plaintext	E	T	A	O	I	N	S	R	H	D
Ciphertext	E	D	T	N	A	R	I	O	S	H

The digraph distribution matrix is shown in Table 9. Now, we will modify putative key as we discussed in swapping procedure. First, we swap the first two elements [9]. New putative key is shown in Table 10. Now, corresponding new putative plaintext will be [9]

```
AOTERTNDSHRITTNAETRIDEOHSOERINTAATASOTTNOETOAAATTSHNEAEEEEEII
```

Diagraph distribution matrix of putative plaintext is shown in Table 11. From the matrix, we can see that, by swapping corresponding row and column we can swap the elements in key.

2.7 Singular Value Decomposition

Properly created metamorphic malware can avoid signature base detection, as well as other detection techniques based on statistical analysis [3]. On the other hand, some techniques based on compression rate, file entropy, and eigenvalue analysis seem to be more precious for malware detection [13]. We want to use such techniques for

Table 11: Corresponding Diagraph Distribution Matrix

	E	T	A	O	I	N	S	R	H	D
E	4	2	1	1	1	0	0	2	0	0
T	1	3	2	1	0	3	1	1	0	0
A	2	2	2	1	0	0	1	0	0	0
O	2	2	1	0	0	0	0	0	1	0
I	0	1	0	0	1	1	0	0	0	1
N	1	1	1	1	0	0	0	0	0	1
S	0	0	0	2	0	0	0	0	2	0
R	0	1	0	0	3	0	0	0	0	0
H	0	0	0	0	0	1	1	1	0	0
D	1	0	0	0	0	0	1	0	0	0

software piracy detection.

Eigenfaces, a technique for facial reorganization is the foundation for this implementation [40]. Singular value decomposition [29] is factorization of the real matrix. The main idea behind the SVD is to consider the high variable dataset and reduce it to the lower dimension dataset in such a way that it clearly defines the substructure of the original dataset [13]. The SVD of the real matrix A yields a factorization of the form

$$A = USV^T.$$

Here, matrix U is the left singular vector of matrix A. U is calculated by the eigenvectors of AA^T. Also, matrix V is the right singular vector of matrix A. V is calculated by the eigenvectors of A^TA. Matrix S is the diagonal matrix. It is calculated by taking the square root of eigenvalues, which is common to both the matrix U and V. UU^T and V^TV are two identity matrices. The eigenvectors of the matrix U is called singular vector because the eigenvector of the matrix U are normalized. Normalization is done by dividing every eigenvector by square root of corresponding eigenvalue. Matrix U contains all eigenvectors as per the singular

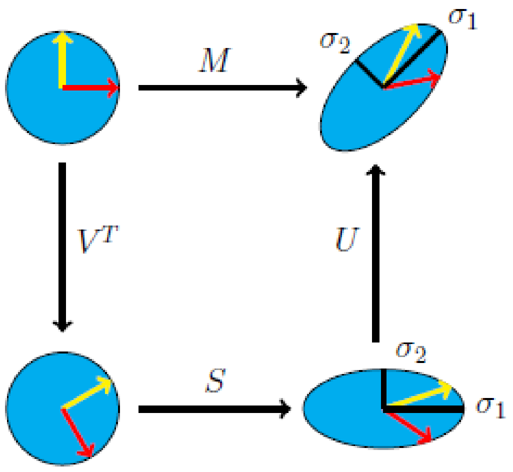

Figure 6: SVD on Matrix A, Matrix Transformation

values of the matrix A. SVD on matrix A is shown in Figure 6 [13].

2.7.1 SVD Algorithm

SVD algorithm can be described in two phases. Training phase followed by testing phase. In the training phase, weights of the input files are determined by projecting them onto eigenspace. In the testing phase, suspected files and benign files are projected onto the eigenspace and their weights are determined. Finally, euclidean distance between the weights of training files and testing files are calculated. Step by step procedure of training phase and testing phase are described below.

2.7.1.1 Training Phase

First, we extract raw bytes from all the input files, and for each of these input files, we construct column vector. Then, the eigenvectors of the covariance matrix were determined. Eigenvectors with low eigenvalues are ignored as they are less important. Then, on eignespace, we project all the files to get weight. This phase is explained as below.

- Get M number of files for training and extract raw bytes. Construct matrix A using the vector of all files.

  $$A = [\phi_1 \phi_2 \phi_3 \ldots \phi_M]. \tag{3}$$

  Suppose, N is the maximum number of bytes an individual file contains, among all files, then matrix A will have N rows. Zeros are appended to column vectors, which contains less than N bytes. To identify variance between different files, eigenvectors of covariance matrix C is determined by

  $$\begin{aligned} C &= \frac{1}{M} \sum_{i=1}^{M} \phi_i \phi_i^T \\ &= AA^T \end{aligned} \tag{4}$$

  In equation (4), M is the number of files.

- Dimensions of matrix A and C are $N \times M$ and $N \times N$ accordingly. It is very hard to find the eigenvectors of such a large matrix. So alternatively we can calculate eigenvectors for another matrix L of dimension $M \times M$. L is calculated using $A^T A$. In following equation (5) v_i is the eigenvector of L and it is calculated using

  $$\begin{aligned} Lv_i &= \lambda_i v_i \\ A^T A v_i &= \lambda_i v_i \end{aligned} \tag{5}$$

  Here, v_i is eigenvector and λ_i is eigenvalue. If we multiply the above equation (5) with A, it will give eigenvectors of matrix C

  $$\begin{aligned} AA^T A v_i &= \lambda_i A v_i \\ CAv_i &= \lambda_i A v_i \end{aligned} \tag{6}$$

  where Av_i is the eigenvector of C. This is called reduce singular value decomposition. Now, according to the eigenvalues, sort the eigenvectors in descending order, because eigenvectors with higher eigenvalues are more important.

- We took M' eigenvectors out of M, where M' is less than M. We project these eigenvectors into the space and space spanned by these vectors are called eigenspace. We can create original software replicate from M' vectors by adding their corresponding weight. Suppose, for software file V in the training set having eigenvectors u_i, we can generate software file as

$$\begin{aligned} V &= w_1 \times u_1 + w_1 \times u_1 + \ldots + w_{M'} \times u_{M'} \\ V &= \sum_{i=1}^{M'} w_i u_i \end{aligned} \tag{7}$$

  Then we can get weight of each file as shown in equation (8) and we can represent set of weight as

$$w_i = \sum_{i=1}^{M'} u_i^T V \tag{8}$$

$$\Omega_i^T = [w_i, w_2, w_3, \ldots, w_{M'}] \tag{9}$$

- The weights of all software files together Δ is shown in equation (10). Weights of all the files together on eigenspace will be the output of the training phase.

$$\Delta = [\Omega_1, \Omega_2, \Omega_3, \ldots \Omega_M] \tag{10}$$

2.7.1.2 Testing Phase

In this phase, we project column vector of each test files on eigenspace. We append zeros to the file that has less than N bytes and remove bytes from the file that is more than N bytes.

$$w_i = \sum_{i=0}^{M'} e_i^T V_n \tag{11}$$

$$\Omega_n^T = [w_1, w_2, w_3, \ldots, w_{M'}] \tag{12}$$

Once we have weight for test files, we compare them with a weight vector of training files. Then, we can calculate euclidean distance between these vectors. If Ω_i

is weight vector for training file then euclidean distance will be

$$\text{distance} = \sqrt{(\omega_1^2 - w_1^2) + (\omega_2^2 - w_2^2) + \ldots + (\omega_1^{M'} - w_1^{M'})} \tag{13}$$

where ω is weight of test file and w is weight of training file.

2.8 Compression-Based Analysis

Utilizing structural entropy analysis is one of the novel approaches for software piracy detection. It has been already used against code obfuscation yielding positive results in [2, 34]. It uses the structural entropy to find variations within the files and calculate a similarity measure. This technique has two major phases: file segmentation followed by sequence comparison. The file segmentation includes entropy measurement with wavelet analysis. Finally, similarity is measured using levenshtein distance.

2.8.1 Structural Entropy

Structural entropy was originally proposed in [34]. It has produced good results for polymorphic malware and metamorphic malware [2, 16]. Unlike other techniques, this technique will not work on opcode sequence; it works on raw byte of the file.

The proposed technique for detection of software piracy is an extension of the technique presented in [2, 16]. Our technique can be divided into two major parts: file segmentation and sequence comparison. File segmentation achieved using Shannon's formula, where entropy is calculated. Once entropy is calculated, wavelet transform is applied [16]. Figure 7 gives the pictorial representation of segmentation process. For sequence comparison, edit distance algorithm is used [16]. Finally, using the similarity formula, the result of the algorithm is compared against the pre-defined threshold.

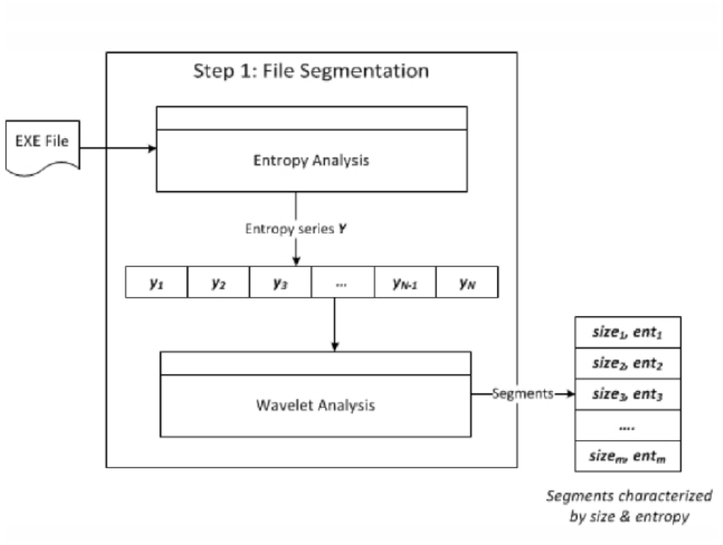

Figure 7: File Segmentation

2.8.2 Classification Based on Compression

Previous research [8] has been done using compression for malware detection. It is based on the principle: given two similar strings, they can be compressed more together than compressed separately. One unknown string is compared against several known strings. Each known string represents unique family. Unknown file is considered of the family with which it best matches [16]. The detection framework is described in the Algorithm 1 and is mentioned in [8].

Detection framework is highly successful. However, the drawback is, memory usage [8] increases rapidly as the size of software increases, which could be a problem in case of very big software.

One another technique based on compression is described in [45]. It depends on detection framework, which uses a learning engine for training on malware and benign code. Using this partial matching phenomenon, two compression models are created. One of these represents the malware code and other represent the benign code. For

Algorithm 1 Kolmogorov Complexity Based Detection Framework

```
1: Input : (1) Training set $TR = \{TR_+, TR_-\}$, where $TR_+$ is set of malware instance, and $TR_-$ is set of benign code instances. (2) Test set , $TE = \{TE_1, \ldots, TE_n\}$, where $TE_i$ is the $i^{th}$ $(i = 1 \ldots n)$ code instance. (3) Estimating function for Kolmogorov complexity, denoted by $K$.
2: Output: Classification $CL(TE_i)\epsilon\{+,-\}$, which corresponds to a benign or malware instance.
3: $M+ \leftarrow K(TR_+)$;
4: $M- \leftarrow K(TR_-))$;
5: for i=1 to n do
6:     $M_i^1 - K(TE_i \cup M+)$;
7:     $Bits(TE_i, M+) = sizeof(M_i^1)$;
8:     $M_i^2 = K(TE_i \cup M-)$;
9:     $Bits(TE_i, M-) = sizeof(M_i^2)$;
10:    $CL(TE_i) = argmin_c\epsilon\{+,-\}Bits(TE_i, M_c)$
11: end for
```

Algorithm 2 PPM Based Classification

```
1: Input : Training set $T = T_+ \cup T_-$, test set $P = \{X_1, \ldots, X_n\}$, and the order of the Markov model in PPM, $k$.
2: Output: Classification of $c(X_i)\epsilon\{+,-\}$ of $X_i\epsilon P$, for $i = 1, \ldots, n$.
3: $M_+ \leftarrow CreatePPM(T_+)$;
4: $M_- \leftarrow CreatePPM(T_-)$;
5: for all $X\epsilon P$ do
6:     $Bits(X, M_+) = ComputeBits(X, M_+)$;
7:     $Bits(X, M_-) = ComputeBits(X, M_-)$;
8:     $c(X) = argmin_c\epsilon\{+,-\}Bits(X, M_c)$;
9: end for
```

any suspected file, average numbers of bits are used to encode it using aforementioned compression model. The suspected file is then classified by the compression rate. Algorithm 2 describes this process.

CHAPTER 3

Implementation

In this section, we discuss about implementation of all techniques. We started with implementation of Hidden Markov Model, followed by Opcode Graph Similarity, Simple Substitution Distance, Singular Value Decomposition, and Compression Based Analysis.

3.1 Implementation of Hidden Markov Model

For training the Hidden Markov Model, we extracted opcode sequences from the base software. Then, we generated five 5% morphed copies of base software using metamorphic generator. All these five files were merged to obtain long observation sequences [20, 44].

Five-fold cross validation was used in this technique. It means, that we divided all files into five subsets. Four subsets were used for training the HMM and remaining one was used as test data [20]. This process is repeated five times; each time testing subset and training subset changes accordingly [20, 44]. Training and scoring phase of HMM is shown in Figure 8.

Secondly, we scored 100 files of each case, that is, 10% morphing to 400% morphing. Then, we scored benign files for comparison. Finally, we plotted ROC curve and AUC.

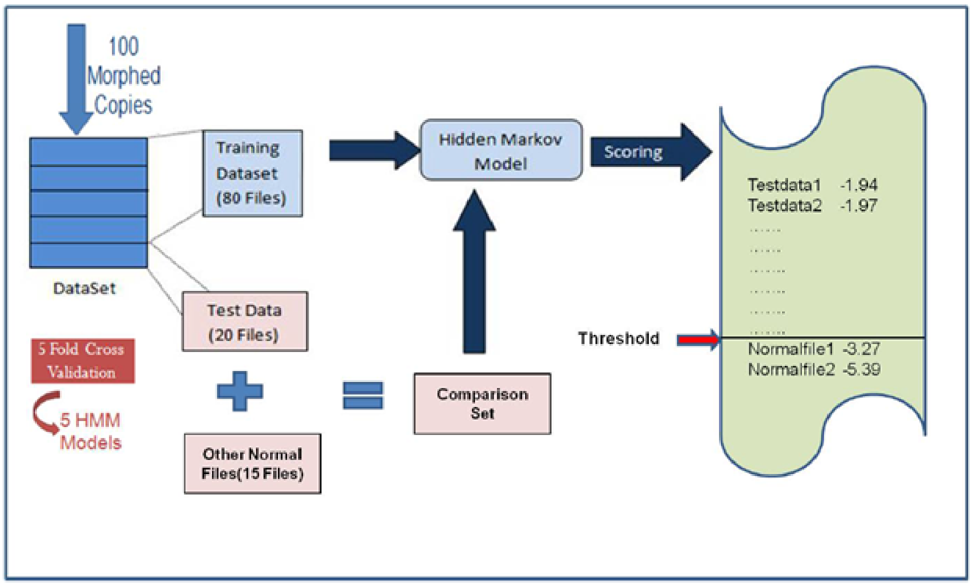

Figure 8: Training and Scoring Phase of HMM

3.2 Implementation of Opcode Graph Similarity

Our goal is to develop the similarity measure from the extracted opcode sequences [26]. First, we extracted the opcode sequence and prepared the weighted directed graph. So far, our technique is similar to the technique used in [1]. But, instead of using graph kernels to generate scores, we directly compared the opcode graphs [26].

Let N be the total number of the distinct opcode from the extracted opcode sequences. We map this opcode to $0, 1, 2, 3, \ldots, N-1$. Let $A = a_{ij}$ and $B = b_{ij}$ be the two edge weighted matrices corresponding to the two executable files (in our case, base software and suspected software), same as Table 5. Note that, both A and B are of size $N \times N$ and both have the same opcode numbering [26]. It means, a_{ij} and b_{ij} represent the opcode i is followed by opcode j corresponds to A and B [26]. In case of different number of distinct opcode in both opcode sequences, we take the superset of distinct opcodes from both sequences. Now, for comparing these matrices, we used following equation.

$$\text{score}(A,B) = \frac{1}{N^2}\left(\sum_{i,j=0}^{N-1} |a_{i,j} - b_{i,j}|\right)^2 \tag{14}$$

If A and B are equal, then minimum score 0 is obtained. If $a_{ij} = 1$ and $b_{jk} = 1$, for $j \neq k$, then maximum possible row sum

$$\sum_{j=0}^{N-1} |a_{i,j} - b_{i,j}| = 2 \tag{15}$$

is obtained [26]. Maximum possible score of 4 is achieved if maximum row sum is achieved for all rows and hence, $0 \leq \text{score}(A,B) \leq 4$.

3.3 Implementation of Simple Substitution Distance

For software piracy detection, we used hill climb technique analogous to Jackobsen's algorithm [12]. The basic idea is that we train the detection system on a sequence of opcodes extracted from a five 5% morphed files and the trained system will be used to score suspected software to determine whether it is pirated or not. In the remainder of this section, we discuss the design of this technique in detail.

We extracted the opcode sequence from suspected software and base software. Using base software we created five 5% morphed files for training. Then, we constructed two digraph distribution matrices, one using suspected file and other using training files. We mapped opcodes to indices $0, 1, 2, 3, \ldots, n-1$. Any opcode other than the top n that occurs in the suspected files or the benign files are grouped together under the same opcode category "Unknown". Let $D = d_{ij}$ and $E = e_{ij}$ be the two digraph distribution matrices of suspected file and training files respectively. The size of both the matrices will be $(n + 1 \times n + 1)$. Both d_{ij} and e_{ij} represent the probability of opcode i followed by opcode j in the suspected file and training files.

We selected initial key K, which best matches with monographic statistics of opcode in the training files. For the experiment, we considered five copies of slightly morphed base software. We assume that most frequent opcode in the training files maps to the most frequent opcode in suspected software, also the second most frequent opcode in training files maps to the second most frequent opcode of suspected software, and so on. We created the D matrix using initial key K, then normalized it by dividing each cell with sum of all cells in matrix.

For constructing E matrix, suppose m denotes number of slightly morphed base files. Then, we can construct m matrices of size $(n+1)\times(n+1)$. We create matrix $F^{(0)}$ with diagraph frequency counts of opcode in training file 0, and $F^{(1)}$ with diagraph frequency counts of opcode in training file 1 and so on. We normalized all the matrices by same way we normalized D matrix [9]. We created E matrix as:

$$E = \{e_{i,j}\} = \left(F^{(0)}_{i,j} + F^{(1)}_{i,j} + \ldots + F^{(m-1)}_{i,j}\right)/m \tag{16}$$

Finally, to compare D and E, we used following equation:

$$\text{score}(k) = d(D,E) = \sum_{i,j} |d_{i,j} - e_{i,j}| \tag{17}$$

In the iterated loop, by swapping the opcode in the key

$$K = \text{opcode}_0, \text{opcode}_1, \text{opcode}_2, \text{opcode}_3, \ldots, \text{opcode}_{n-1}, \text{opcode}_{\text{unknown}}$$

we changed the putative key, and the swapping is done the same way as in Jackobsen's method [12]. In first iteration, all the opcode away from a distance of one are swapped, that is opcode$_0$ with opcode$_1$ and so on. In the second iteration, all the opcode away from a distance of two are swapped, that is, opcode$_0$ with opcode$_2$, and so on. Finally, in the n^{th} iteration, all the opcode away from distance of n are swapped, that is, opcode$_0$ with opcode$_n$. After each swapping, we computed the score by comparing D matrix with E. If the score improves, we update the putative key and start over again from the first iteration [9]. If the score does not improve, then we do other modification with the old key. We continue swapping for $\binom{n}{2}$ iterations to ensure all $\binom{n}{2}$ pairs of opcodes in key are swapped at least once [9, 27]. Finally, we scored, 100 files of each cases, that is 10% morphing to 400% morphing and plotted ROC curve and AUC.

3.4 Implementation of Singular Value Decomposition

We extracted raw bytes from the text section of training files and constructed a training input matrix A. If we have M files for training and Maximum number of bytes among all files is N then matrix A will be of size $N \times M$. Zeros are append to the files, which has fewer bytes than N and first N bytes are taken from the files that have more than N bytes.

This matrix is passed to the JAMA API (JAVA Matrix Package), which is developed in JAVA for the calculation of singular vectors and singular values. Using these singular vectors, we have calculated the weights of training files [13]. Weights for the testing files are calculated by projecting their column vectors on singular space. Once we have the weights for both training set files and testing set files, we can measure the euclidean distance between the calculated weights. Figure 9 is the graphical representation of the process.

3.5 Implementation of Compression-Based Analysis

Implementation of compression based analysis has two major phases, File Segmentation followed by Sequence Comparison. File Segmentation phase measures the data complexity throughout the file using structural entropy and Sequence Comparison measures the similarity between files.

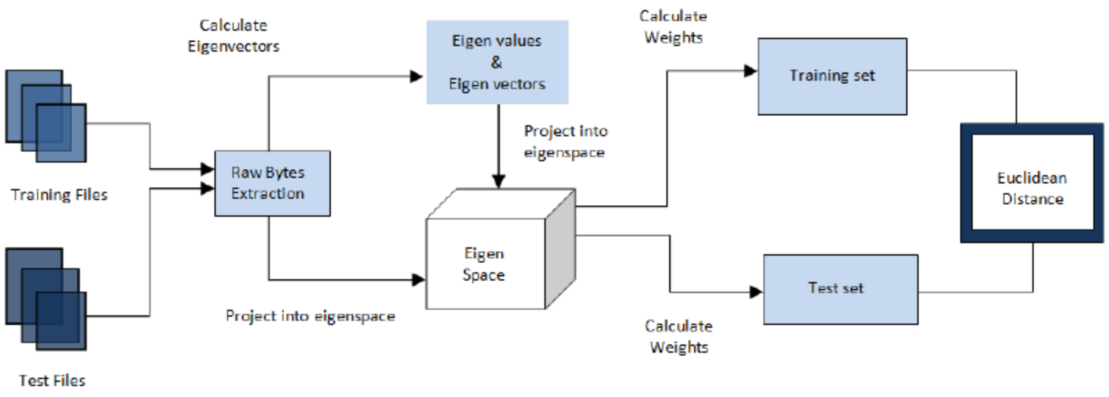

Figure 9: Process of Singular Value Decomposition

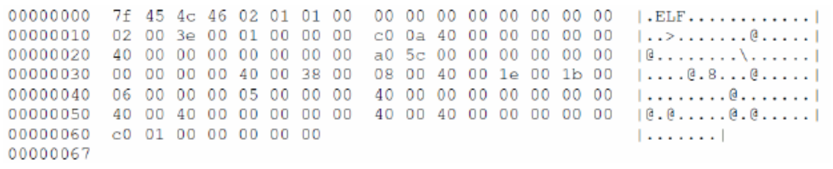

```
00000000  7f 45 4c 46 02 01 01 00  00 00 00 00 00 00 00 00  |.ELF............|
00000010  02 00 3e 00 01 00 00 00  c0 0a 40 00 00 00 00 00  |..>.......@.....|
00000020  40 00 00 00 00 00 00 00  a0 5c 00 00 00 00 00 00  |@........\......|
00000030  00 00 00 00 40 00 38 00  08 00 40 00 1e 00 1b 00  |....@.8...@.....|
00000040  06 00 00 00 05 00 00 00  40 00 00 00 00 00 00 00  |........@.......|
00000050  40 00 40 00 00 00 00 00  40 00 40 00 00 00 00 00  |@.@.....@.@.....|
00000060  c0 01 00 00 00 00 00                              |.......|
00000067
```

Figure 10: Sample File and It's Hexdump

3.5.1 Creating File Segments

In this section we discuss about splitting the files into windows and then calculating the compression ratio for each window. Finally, wavelet transformation is applied in order to get smoothed data.

3.5.1.1 Splitting Files Into Byte Windows

First of all, this technique splits file into byte windows. These windows are strings of consecutive bytes, nearly the same size in terms of bytes. As we are considering file as a single stream of data, we should overlap windows to some extent. Window size and its slide size are determined experimentally [16]. As shown in the hex dump of sample file in Figure 10 [16], the file contains 103 bytes.

For example, the window size is 10 bytes and windows slide size is 5 bytes. The first window is shown in Figure 11 and the second window is shown is Figure 12.

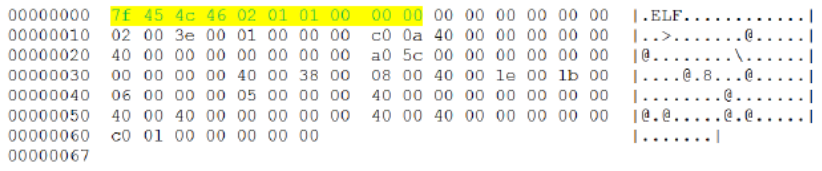

```
00000000  7f 45 4c 46 02 01 01 00  00 00 00 00 00 00 00 00  |.ELF............|
00000010  02 00 3e 00 01 00 00 00  c0 0a 40 00 00 00 00 00  |..>.......@.....|
00000020  40 00 00 00 00 00 00 00  a0 5c 00 00 00 00 00 00  |@........\......|
00000030  00 00 00 00 40 00 38 00  08 00 40 00 1e 00 1b 00  |....@.8...@.....|
00000040  06 00 00 00 05 00 00 00  40 00 00 00 00 00 00 00  |........@.......|
00000050  40 00 40 00 00 00 00 00  40 00 40 00 00 00 00 00  |@.@.....@.@.....|
00000060  c0 01 00 00 00 00 00                              |.......|
00000067
```

Figure 11: Sample File and It's Windows1

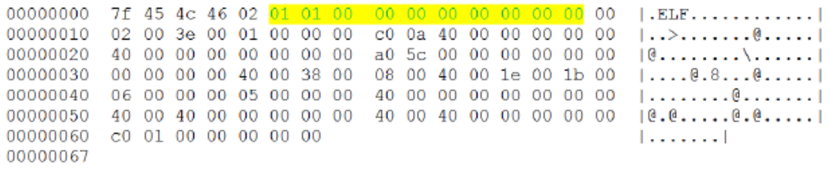

```
00000000  7f 45 4c 46 02 01 01 00  00 00 00 00 00 00 00 00  |.ELF............|
00000010  02 00 3e 00 01 00 00 00  c0 0a 40 00 00 00 00 00  |..>.......@.....|
00000020  40 00 00 00 00 00 00 00  a0 5c 00 00 00 00 00 00  |@........\......|
00000030  00 00 00 00 40 00 38 00  08 00 40 00 1e 00 1b 00  |....@.8...@.....|
00000040  06 00 00 00 05 00 00 00  40 00 00 00 00 00 00 00  |........@.......|
00000050  40 00 40 00 00 00 00 00  40 00 40 00 00 00 00 00  |@.@.....@.@.....|
00000060  c0 01 00 00 00 00 00                              |.......|
00000067
```

Figure 12: Sample File and It's Windows2

All the remaining windows are measured the same way. If the final window contains fewer bytes than the window size, null byte are appended [16].

In reality the windows size should be larger to derive any meaningful information from compression analysis. On the other hand, size should not be too large that it could allow attackers to mask any malicious code.

3.5.1.2 Compression Ratios for Windows

Having numbers of window, we need to calculate their compression ratio. The vital part is that, windows with low entropy data should have higher compression ratio and windows with high entropy data should have lower compression ratio. Therefore, without having actual code, compression ratio gives us information about the underlying part of the file.

To calculate compression ratios, we used the software application named gzip. The main algorithm behind the gzip is lempel-ziv (LZ77) [16]. This algorithm measures the distribution of unique byte sequence in the window. Figure 13 show, the compression ratio derived from an example file.

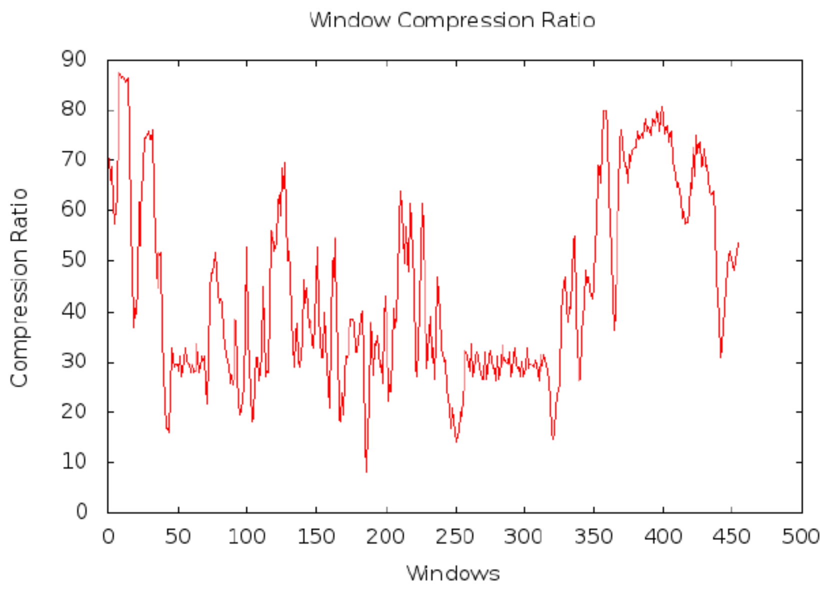

Figure 13: Window Compression Ratio of Sample File

3.5.1.3 Wavelet Transform Analysis

In the Figure 13, we can see that data can vary rapidly and it would be very hard to compare sets of plot. Using wavelet transformation, data can be smoothed where highly variations occur. In our implementation, we choose discrete Haar wavelet transform [16] from various wavelet transforms. We decided to choose it from previous work [2, 34]. This transforms gives simple and efficient results. Suppose, we have N values: $x = (x_1, x_2, \ldots, x_N)$. Here, N is even number. s_k and d_k will be determined as

$$s_k = \frac{x_{2k-1} + x_{2k}}{2} \tag{18}$$

and

$$d_k = \frac{x_{2k} - x_{2k-1}}{2} \tag{19}$$

respectively. Discrete Haar wavelet transform can then be determined by [10]

$$x = (x_1, ..., x_N) \rightarrow (x|d) = (s_1, \ldots, x_{N/2}|d_1, \ldots, d_{N/2}) \tag{20}$$

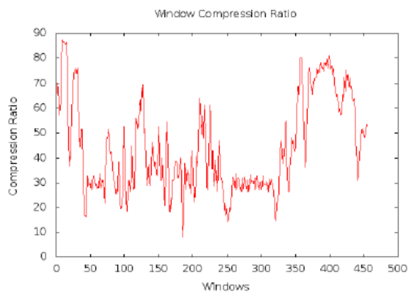

(a)

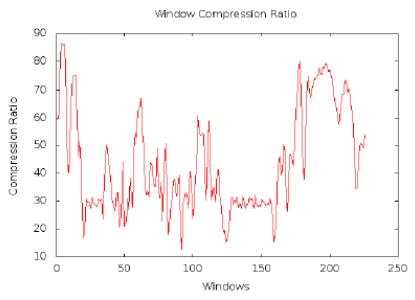

(b)

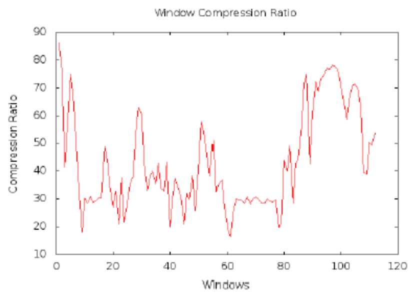

(c)

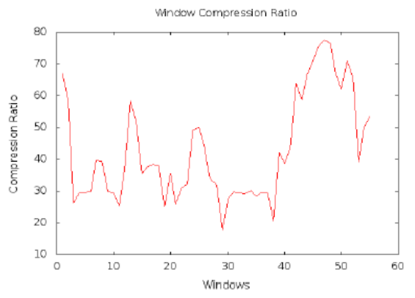

(d)

Figure 14: Wavelet Transform for 0 Iteration, 1 Iteration, 2 Iteration and 3 Iteration Respectively

The s_k contains set of values, known as pair-wise averages. We can perform discrete haar wavelet transform recursively and arbitrary times of iteration. The transform can only be applicable to sets, which contains even values. For the set, which contains an odd value, we need to pad last value to pretend as original data. Figure 14 shows the effect of three iterations on data.

3.5.1.4 Creation of File Segment

Next, we want to form the file segments. For that, we need threshold, which determine that which is high entropy and which is a low entropy [16]. In our experiment, we decided 0.65 as a threshold after examining calibration experiment [16]. So, values of compression ratio greater than 0.65 considered low entropy and values less than 0.65 are considered high entropy [16].

Table 12: Final File Segments

Segment #	Segment Length	Segment Value
1	1	0.820
2	1	0.640
3	3	0.897
4	2	0.575
5	3	0.903

Now, every segment has a length and value associated with it. Segment length represents all the values of compression ratio, contributing to a particular segment. The mean of all associated ratios are considered as the segment value. For example, suppose the final wavelet transformed values are 0.82, 0.64, 0.79, 0.90, 1.00, 0.60, 0.55, 0.93, 0.88, 0.90. Considering threshold of 0.65, Table 12 shows the resulting segment.

3.5.2 Comparison Between Sequences

The final sequence of segments represents a particular file. Now, the problem of file similarity becomes the problem of sequence comparison. For comparison, we used the levenshtein distance based algorithm. Finally, to determine the similarity we used the distance between the sequences. This approach is derived from [2, 34].

3.5.2.1 Levenshtein Distance

To measure the difference between two files, a string metric named levenshtein distance is used [42]. It is also called the edit distance. Specifically, the levenshtein distance is the number of operations that need to be performed like insertion, deletion and substitution to convert a into b [6]. Lesser the operation, the more similar strings are. For demonstration, we took two string `abcde` and `azbcy`. Assume the cost of each operation, insertion, deletion and substitution as 1. Then, to convert `abcde` to `azbcy`,

$$\text{abcde} \to \text{azbcde (insert } \texttt{z}\text{)}$$

$$\text{azbcde} \to \text{azbcye (substitute } \texttt{d} \text{ for } \texttt{y}\text{)}$$

$$\text{azbcye} \to \text{azbcy (delete } \texttt{e}\text{)}$$

Since three operations are the minimum number of edits required to convert abcde to azbcy, the Levenshtein distance between these two strings is considered as three. Various combinations of operation is possible.

To generalize the process, if two sequences are $X = (x_1, x_2, \ldots, x_n)$ and $Y = (y_1, y_2, \ldots, y_m)$, and cost of the functions are predefined than we can obtain the matrix of elements. Using the following recursion (21) elements of the matrix

$$D_{(n+1)\times(m+1)} = \{d_{i,j}\}$$

are computed as [2]

$$d_{i,j} = \begin{cases} 0 & \text{if } i = j = 0 \\ d_{0,j-1} + \delta_y(j) & \text{if } i = 0 \text{ and } j > 0 \\ d_{i-1,0} + \delta_x(i) & \text{if } i > 0 \text{ and } j = 0 \\ d_{i-1,j-1} & \text{if } x_i = y_j \\ \min \begin{cases} d_{i,j-1} + \delta_y(j) \\ d_{i-1,j} + \delta_x(i) \\ d_{i-1,j-1} + \delta_{X,Y}(i,j)) \end{cases} & \text{if } x_i \neq y_i \end{cases} \tag{21}$$

Here,

$$\delta_Y(j) = \text{cost of insertion}$$

$$\delta_X(i) = \text{cost of deletion}$$

$$\delta_{X,Y}(i,j) = \text{cost of substitution}$$

Considering the cost of δ_Y, δ_Y and $\delta_{X,Y}$ as 1 and using it with equation (21) for calculating the levenshtein distance for abcde and azbcy example, we get the matrix as shown in Table 13. The $d_{n,m}$ gives the final score of the distance.

Table 13: Edit Matrix for Both Strings

		a	b	c	d	e
	0	1	2	3	4	5
a	1	0	1	2	3	4
z	2	1	1	2	3	4
b	3	2	1	1	2	3
c	4	3	2	1	2	3
y	5	4	3	2	2	3

3.5.2.2 Sequence Alignment

Suppose we have X and Y, two different files for similarity calculation. Then we derived respective segment x_i for $i = 1, 2, 3, \ldots, n$ and y_i for $j = 1, 2, 3, \ldots, m$ as per the segmentation process. We used the cost function mentioned in [2, 34] to account for size differences.

$$\text{cost}_\sigma(x_i, y_j) = \frac{|\sigma(x_i) - \sigma(y_j)|}{\sigma(x_i) + \sigma(y_j)} \tag{22}$$

Here, $\delta_Y(j)$ is size of segment x_i and $\delta_X(i)$ is size of segment y_j.

The possible range of cost function is between 0 and 1 inclusively. We use following cost function mentioned in [2, 34] with respect to compression ratio differences.

$$\text{cost}_\epsilon(x_i, y_j) = \frac{1}{1 + e^{-4|\epsilon(x_i) - \epsilon(y_j) + 6.5|}} - 0.001501 \tag{23}$$

Here, $\epsilon(x_i)$ and $\epsilon(y_j)$ = compression ratios of respective segments. Two constant 6.5 and 0.001501 helps to produce the value of $cost_\epsilon$ between 0 and 1 [2]. Using equations (22) and (23), the final version of the cost function is

$$\text{cost}(x_i, y_j) = c_\sigma \ \text{cost}_\sigma(x_i, y_j) + c_\epsilon \ \text{cost}_\epsilon(x_i, y_j) \tag{24}$$

Here, c_σ is constant for size and c_ϵ is constant for entropy cost.

The cost function (24) applies to sequence alignment algorithm, which is based on levenshtein distance. Using dynamic programming, two-dimensional array similar to Table 13 is created. Finally, got the last element for cost calculation between two-segment sequences [16]. To use, equation (21) for calculating elements of the array, we make $\tau = 0.3$ and prepared functions

$$\begin{aligned} \delta_Y(j) &= \tau \ \log \sigma(y_{j-1}) \\ \delta_X(i) &= \tau \ \log \sigma(x_{i-1}) \\ \delta_{X,Y}(i,j) &= \text{cost}(x_{i-1}, y_{j-1}) \log \left(\frac{\sigma(x_{i-1}) + \sigma(y_{j-1})}{2} \right) \end{aligned} \tag{25}$$

The functions in (25) are derived in [2]

3.5.2.3 Similarity Calculation

Once we have calculated edit distance using equation (21) with penalty functions (25), we can calculate similarity between file X and Y using [16]

$$\text{similarity} = 100 \left(1 - \frac{d_{n,m}}{\text{cost}_{\max}} \right) \tag{26}$$

Here, $\text{cost}_{\max}$ is worst case penalty and it is calculated in a special way as follow by considering penalty functions (28).

$$\text{cost}_{\max} = d'_{0,m} + d'_{n,0} \tag{27}$$

$$\begin{aligned} \delta'_Y(j) &= \delta_Y(j) \\ \delta'_X(i) &= \delta_X(i) \\ \delta'_{X,Y}(i,j) &= 2\tau \left(\log \sigma(x_{i-1}) + \log \sigma(y_{j-1}) \right) \end{aligned} \tag{28}$$

CHAPTER 4

Experimental Results

In all of the techniques we experimented, our main goal is to verify that, whether our techniques are able to distinguish between pirated software and legitimate software. We experimented with 10% of morphed files to 400% of morphed files. For each technique, we tried to find the point (morphing percentage) where techniques stop giving the ideal results. Finally, we plotted receiver operating characteristic curve (ROC) and area under the curve (AUC) for each case. We used cygwin utilities files as benign files and generated morphed copies using the metamorphic generator.

4.1 Hidden Markov Model

In our experiment, we found that up to 70% of morphing HMM is able to distinguish between pirated software and legitimate software. From 80% onwards, technique is not able to distinguish properly. It happens because, as we add more deadcode, morphed files become more similar to the benign files and less similar to the original base software. We can clearly observe this in Table 14 of the AUC.

4.2 Opcode Graph Similarity

In our experiment, we found that up to 80% of morphing this technique is able to distinguish clearly between pirated software and legitimate software. This means that AUC remains 1 till 80% of morphing. For 90% and 100% of morphing AUC remains in the range of 0.9, which shows that this technique is able to distinguish until 100% of morphing. From the 300% onwards the technique is failing totally. It happens because, as we added more number of deadcode, morphed files start losing

Table 14: AUC - Hidden Markov Model

Morphing Percentage(%)	AUC
10	0.80937
20	0.745
30	0.71937
40	0.62313
50	0.6125
60	0.51562
70	0.51
80	0.51
90	0.3575
100	0.38813
200	0.20313
300	0.15188
400	0.1325

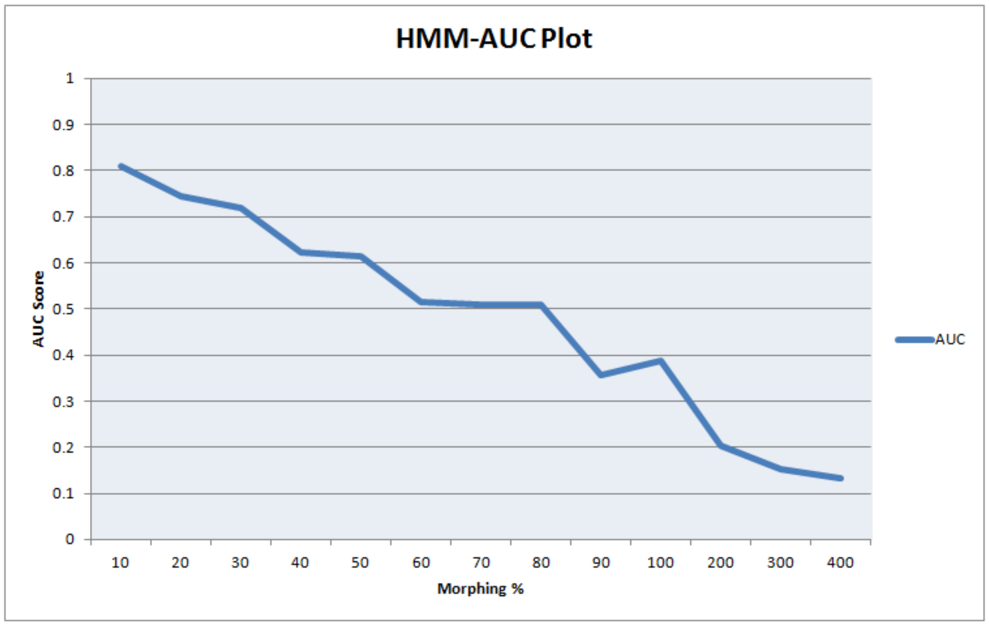

Figure 15: Hidden Markov Model AUC Plot

its originality from base software. We can clearly observe this in Table 15 for the AUC.

Table 15: AUC - Opcode Graph Similarity

Morphing Percentage (%)	AUC
10	1
20	1
30	1
40	1
50	1
60	1
70	1
80	1
90	0.96562
100	0.90250
200	0.17625
300	0
400	0

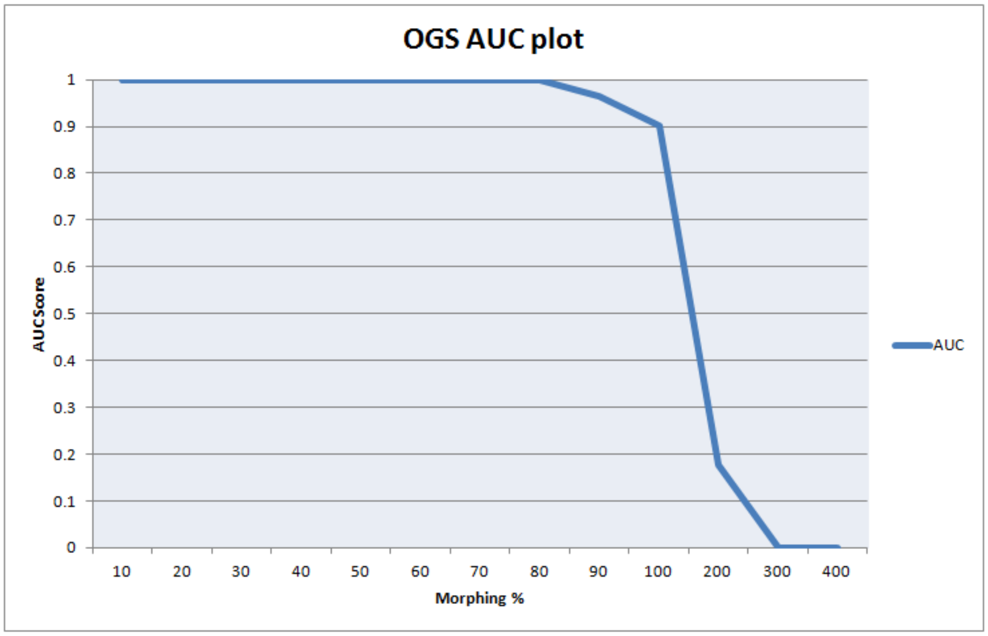

Figure 16: Opcode Graph Similarity AUC Plot

4.3 Simple Substitution Distance

In our experiment, we found that up to 100% of morphing this technique is able to clearly distinguish between pirated software and legitimate software. This means

Table 16: AUC - Simple Substitution Distance

Morphing Percentage (%)	AUC
10	1
20	1
30	1
40	1
50	1
60	1
70	1
80	1
90	1
100	1
200	0.996
300	0.896
400	0.856

that AUC remains 1 until 100% of morphing. From 200% to 400% morphing AUC remains in the range of 0.9 - 0.8, which shows that the technique is able to distinguish up to that range. So, in our experiment up to 400% of morphing, which is the highest percentage of morphing we experimented with, the technique is not failing completely. We can clearly observe this in Table 16 for the AUC.

4.4 Singular Value Decomposition

In our experiment, we found that up to 50% of morphing, this technique is able clearly to distinguish between pirated software and legitimate software. This means that the AUC remains 1 until the 50% of morphing. From 60% to 400% morphing AUC remains in the range of 0.99 - 0.91, which shows that this technique is still able to distinguish in that range with clarity. So, in our experiment up to 400% of morphing, which is the highest percentage of morphing we experimented with, the technique is giving good results. We can clearly observe this in Table 17 for the AUC.

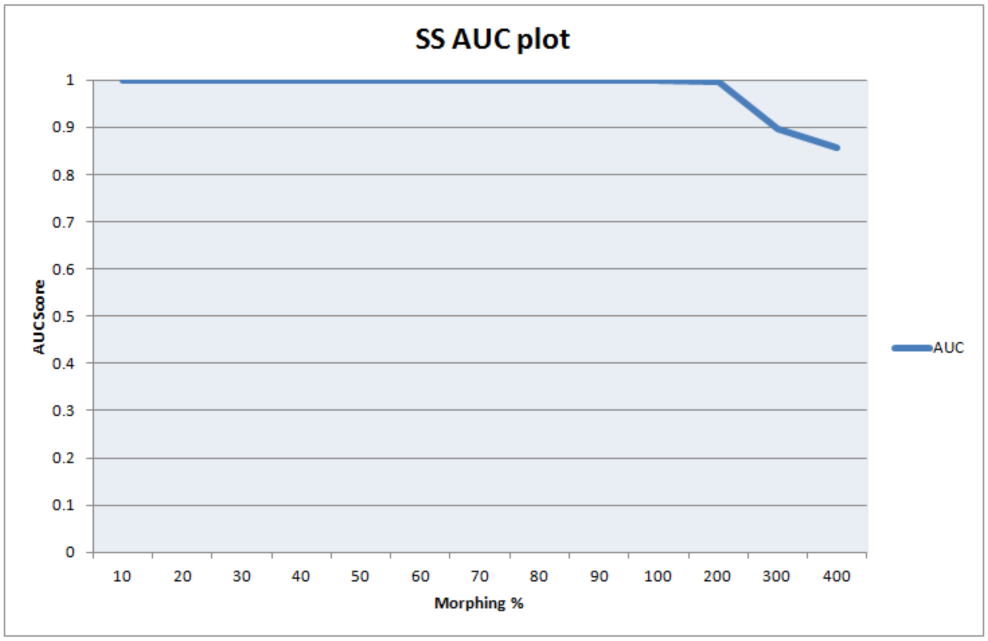

Figure 17: Simple Substitution Distance AUC Plot

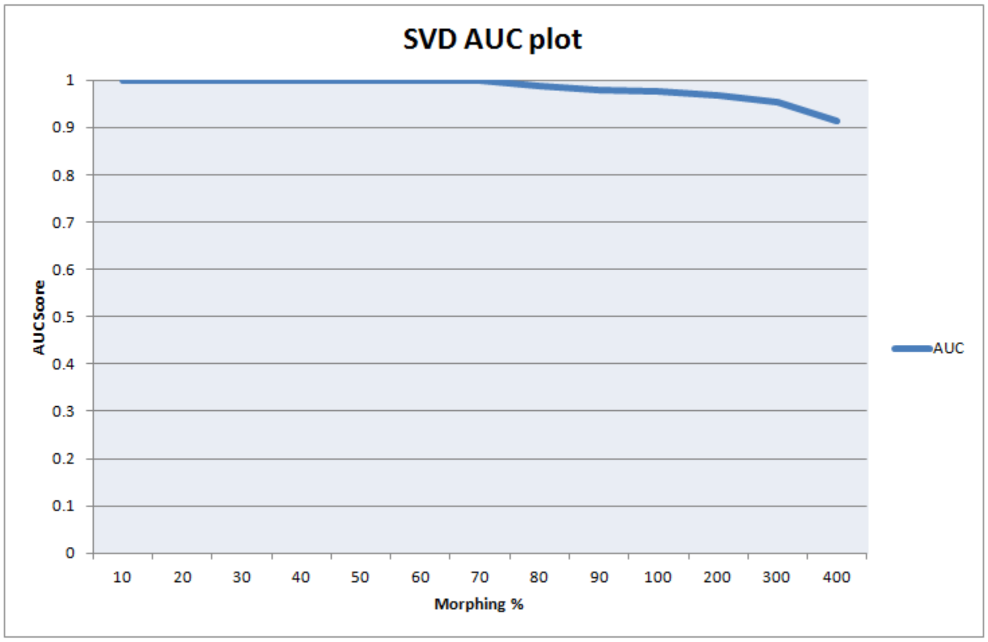

Figure 18: Singular Value Decomposition AUC Plot

Table 17: AUC - Singular Value Decomposition

Morphing Percentage (%)	AUC
10	1
20	1
30	1
40	1
50	1
60	0.99999
70	0.99769
80	0.98834
90	0.97959
100	0.97665
200	0.96776
300	0.95406
400	0.91427

4.5 Compression-Based Analysis

In our experiment, we found that up to 90% of morphing this technique is able to clearly distinguish between pirated software and legitimate software. This means that AUC remains 1 until 90% of morphing. From 100% to 400% morphing AUC remains in the range of 0.9 - 0.8, which shows that the technique is able to distinguish up to that range. So, in our experiment up to 400% of morphing, which is the highest percentage of morphing we experimented with, the technique is not failing completely. We can clearly observe this in Table 18 for the AUC.

Roc curves for all the methods are shown in the Appendix.

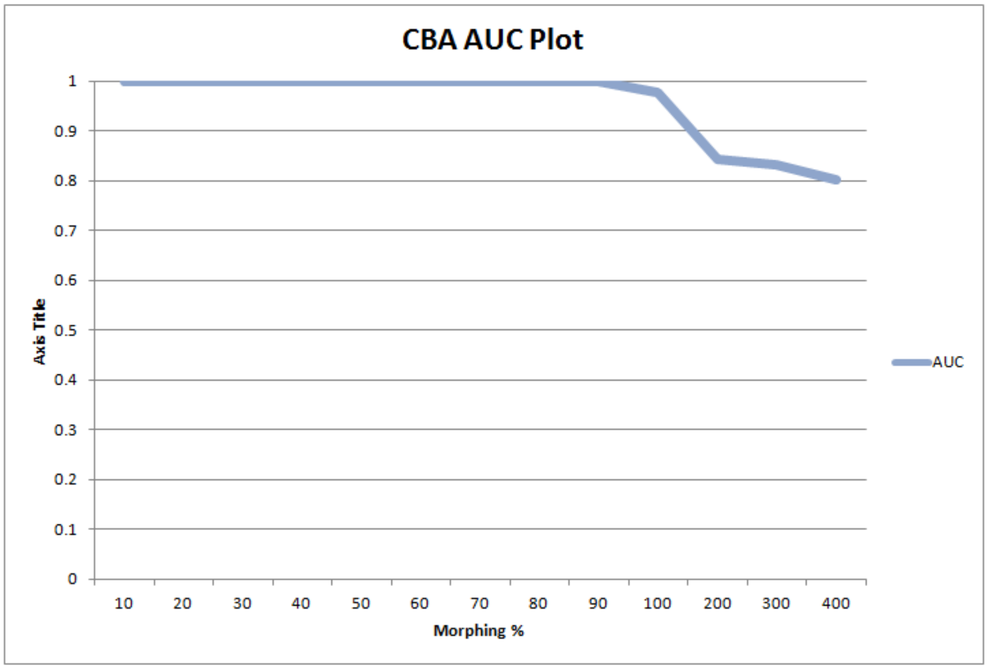

Figure 19: Compression-Based Analysis AUC Plot

Table 18: AUC - Compression-Based Analysis

Morphing Percentage (%)	AUC
10	1
20	1
30	1
40	1
50	1
60	1
70	1
80	1
90	1
100	0.97823
200	0.84218
300	0.83129
400	0.80136

CHAPTER 5
Conclusion and Future Work

All the techniques we discussed in the paper were previously used to detect metamorphic malware. In this paper, we proposed these techniques for the completely different approach of software piracy detection. We wrote our own metamorphic generator to replicate suspected software. Input to the metamorphic generator are numbers of the suspected software and amount of morphing percentage, and it will replicate suspected software accordingly. We used cygwin utilities files as benign files. First three techniques that are based on statistical analysis work on the disassembled files whereas last two techniques work directly on raw bytes of the file.

Our experimental results show that all the techniques are robust in detecting pirated software. The Hidden Markov Model is able to distinguish between pirated software and legitimate software up to 70% of morphing. The AUC for HMM falls gradually with morphing percentage. The opcode graph similarity method is able to distinguish up to 100% of morphing, Up to 80% it is distinguishing with 0% false positive and 0% false negative, which means AUC is 1 up to 80% . Over 100% of morphing AUC falls exponentially. Simple substitution distance is able to distinguish clearly up to 100% of morphing, that is with 0% false positive and 0% false negative. In singular value decomposition AUC is 1 up to 50% and in the range of 0.9 from 60% onward. Lastly, in Compression-based analysis AUC is 1 up to 100% and start falling from 200% onward.

For future work, one can try other morphing techniques than dead code insertion, like code permutation and instruction replacement. Morphing using the instruction replacement technique could be hard to detect because instead of changing the code sequence or inserting some dead code, it actually changes the code. In addition, one can experiment with different types of files. Throughout our project, we experimented with executable files (.exe files), but one can experiment with other types like byte code. Various new metamorphic malware are coming into the market daily, so by observing them one can generate some challenging suspected software to experiment with.

This project can be extended by combining both static and dynamic birthmarks. All the techniques we experimented with are considered as static birthmark as they work on statistically available information. In contrast, dynamic birthmark work on information gathered by executing the program.

Finally, the results of all the techniques, we experimented with can be improved for a higher amount of morphing.

LIST OF REFERENCES

[1] Anderson, B.: Graph-Based Malware Detection Using Dynamic Analysis. *Journal in Computer Virology*, 7(4) 247–258 (2011).

[2] Baysa, D., Low, R.M., Stamp, M.: Entropy And Metamorphic Malware. *Journal of Computer Virology and Hacking Techniques*, 9(4) 179–192 (2013).

[3] Borello, J., Me, L.: Code Obfuscation Techniques For Metamorphic Viruses. *Journal in Computer Virology*, 4(3) 30–40 (2008).

[4] Cesare, S.: Fast Automated Unpacking And Classification Of Malware. Masters Thesis, Central Queensland University. Retrieved from `http://acquire.cqu.edu.au:8080/vital/access/manager/Repository/cqu:7351`

[5] Computer Virus Creation kit. Retrived from `http://www.informit.com/articles/article.aspx?p=366890&seqNum=6`

[6] Cormode, G., Muthukrishnan, S.: The String Edit Distance Matching Problem With Moves. *Journal in Association for Computing Machinery Transactions on Algorithms*, 3(2) (2007). Retrieved from `http://dimacs.rutgers.edu/~graham/pubs/papers/editmoves.pdf`

[7] Costello, F., Bleakley, C., Aliefendic, S.: Using Whitespace Patterns To Detect Plagiarism In Program Code. Retrieved from `http://www.csi.ucd.ie/content/using-whitespace-patterns-detect-plagiarism-program-code`

[8] Deng, W., et al: A Malware Detection Framework Based On Kolmogorov Complexity. *Journal of Computational Information Systems*, 7(8) 2687–2694 (2011). Retrieved from `http://www.jofcis.com/publishedpapers/2011_7_8_2687_2694.pdf`

[9] Dhavare, A., Low, R., Stamp, M.: Efficient Cryptanalysis Of Homophonic Substitution Ciphers. *Cryptologia*, 37(3) 250–281 (2013).

[10] Fleet, P.: The Discrete Haar Wavelet Transformation. *Joint Mathematical Meetings*, (2007). Retrieved from `http://cam.mathlab.stthomas.edu/wavelets/pdffiles/NewOrleans07/HaarTransform.pdf`

[11] Gao, X., Stamp, M.: Metamorphic Software For Buffer Overflow Mitigation. *In Proceedings of the 2005 Conference on Computer Science and its Applications*, Retrieved from `http://www.cs.sjsu.edu/faculty/stamp/papers/BufferOverflow.doc`

[12] Jakobsen, T.: A Fast Method For The Cryptanalysis Of Substitution Ciphers. *Cryptologia*, 19 265–274 (1995).

[13] Jidigam, R., et al: Metamorphic Detection Using Singular Value Decomposition. Master's Project, San Jose State University, Paper 330, (2013). Retrieved from `http://scholarworks.sjsu.edu/etd_projects/330`

[14] Kazi, S., Stamp, M.: Hidden Markov Models For Software Piracy Detection. *Information Security Journal: A Global Perspective*, 22(3) 140–149 (2013).

[15] Konstantinou, E.: Metamorphic Virus: Analysis and Detection. Technical Report, Royal Holloway, University of London. Retrieved from `http://www.ma.rhul.ac.uk/static/techrep/2008/RHUL-MA-2008-02.pdf`

[16] Lee, J.: Compression-Based Analysis Of Metamorphic Malware. Master's Projects, San Jose State University, Paper 329, (2013). Retrieved from `http://scholarworks.sjsu.edu/etd_projects/329`

[17] Lukashenko, R., Graudina, V., Grundspenkis, J.: Computer-Based Plagiarism Detection Methods And Tools: An Overview. *In Proceedings of the 2007 International Conference on Computer Systems and Technologies*, (2007).

[18] Mathai, J.: History Of Computer Cryptography And Secrecy System. Retrieved from `http://www.dsm.fordham.edu/~mathai/crypto.html`

[19] Muhaya, F., Khan M. K., Xian, Y.: Polymorphic Malware Detection Using Hierarchical Hidden Markov Model. *In Proceedings of the 2011 IEEE Ninth International Conference on Dependable, Autonomic and Secure Computing*, 151–155 (2011).

[20] Mungale, M.: Robust Watermarking Using Hidden Markov Models. Master's Projects, San Jose State University, Paper 179, (2011). Retrieved from `http://scholarworks.sjsu.edu/etd_projects/179`

[21] Mungale, M., Stamp, M.: Software Similarity and Metamorphic Detection. *In Proceedings of 2012 International Conference on Security and Management*, (2012).

[22] Myles, G., Collberg, C.: Detecting Software Theft Via Whole Program Path Birthmarks. *Information Security ISC 2004 7th International Conference*, 404–415 (2004).

[23] Rad, B., Masrom, M.: Metamorphic Virus Variants Classification Using Opcode Frequency Histogram. *In Proceedings of the 14th WSEAS International Conference on Computers*, 147–155 (2010).

[24] Raysman, R., Brown, P.: Copyright Infringement Of Computer Software And The Altai Test. *New York Law Journal*, 235(89) (2006).

[25] Rigoll, G.: Maximum Mutual Information Neural Networks For Hybrid Connectionist HMM Speech Recognition Systems. *IEEE Transactions on Speech and Audio Processing*, 175–184 (1994).

[26] Runwal, N., Low, R., Stamp, M.: Opcode Graph Similarity And Metamorphic Detection. *Journal in Computer Virology*, 8(1-2) 37–52 (2012).

[27] Shanmugam, G.: Simple Substitution Distance And Metamorphic Detection.*Journal of Computer Virology and Hacking Techniques*, 9(3) 159-170 (2013).

[28] Si, A., Leong, H.V., Lau, R.W.H.: A Document Plagiarism Detection System. *In Proceedings of the 1997 Association for Computing Machinery Symposium on Applied Computing*, 70–77 (1997).

[29] Singular Value Decomposition. *Wolfram MathWorld*, Retrived from `http://mathworld.wolfram.com/SingularValueDecomposition.html`

[30] Software Piracy. Retrived from `http://www.bsa.org/anti-piracy`

[31] Software Piracy Study. Retrived from `http://globalstudy.bsa.org/2010/downloads/study_pdf/2010_BSA_Piracy_Study-Standard.pdf`

[32] Software Piracy On The Internet: A Threat To The Security. Retrived from `http://portal.bsa.org/internetreport2009/2009internetpiracyreport.pdf`

[33] Software Piracy. Retrived from `http://www.microsoft.com/en-us/piracy/default.aspx`

[34] Sorokin, I.: Comparing Files Using Structural Entropy. *Journal in Computer Virology*, 7(4) 259–265 (2011).

[35] Stamp, M.: A Revealing Introduction To Hidden Markov Models. (2004). Retrived from `http://www.cs.sjsu.edu/~stamp/RUA/HMM.pdf`

[36] Stamp, M.: *Information Security: Principles And Practice*, Second Edition, Wiley (2011).

[37] Stamp, M.: Risks Of Monoculture. *Communications of the Association for Computing Machinery Homeland Security*, 47(3) 120 (2004).

[38] Sudarshan, M.S., Stamp, M.: Metamorphic Worm That Carries Its Own Morphing Engine. *Journal in Computer Virology*, 9(2) 49–58 (2013).

[39] Tamada, H.S., Okamoto, K., Nakamura, M., Monden, A., Matsumoto, K.-I.: Dynamic Software Birthmarks To Detect The Theft Of Windows Applications. *In International Symposium on Future Software Technology*, (2004).

[40] Turk, M.A., Pentland, A.P.: Eigenfaces For Recognition. *Journal of Cognitive Neuroscience*, 3(1) 71–86 (2007).

[41] Venkatesan, A., Stamp, M.: Code Obfuscation And Virus Detection. Master's Project, San Jose State University, Paper 116 (2008). Retrived from `http://scholarworks.sjsu.edu/etd_projects/116`

[42] Wagner, R.A., Fischer, M.J.: The String-To-String Correction Problem. *Journal of the Association for Computing Machinery*, 21(1) 168–173 (1974). Retrived from `http://www.inrg.csie.ntu.edu.tw/algorithm2013/homework/Wagner-74.pdf`

[43] Wikipedia, Hill Climbing Retrived from `http://en.wikipedia.org/wiki/Hill_climbing`

[44] Wong, W., Stamp, M.: Hunting For Metamorphic Engines. *Journal in Computer Virology*, 2(3) 221–229 (2006).

[45] Zhou, Y., Inge, M.: Malware Detection Using Adaptive Data Compression. *Proceedings of the 1st Association for Computing Machinery Workshop on AISec*, 53–60 (2008).

APPENDIX

ROC Curve

A.1 ROC Curve for Hidden Markov Model

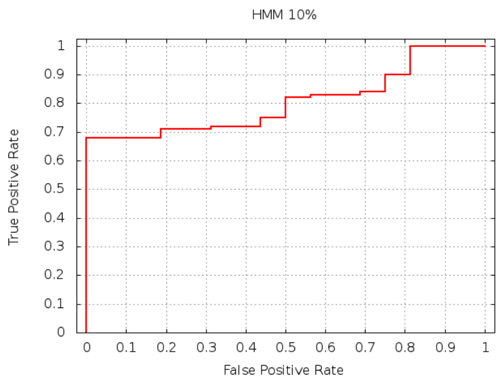

Figure A.1: ROC for HMM 10% morphing

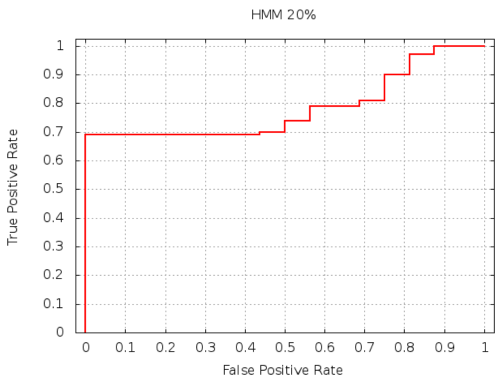

Figure A.2: ROC for HMM 20% morphing

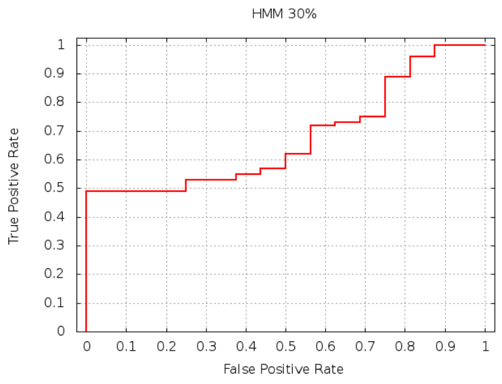

Figure A.3: ROC for HMM 30% morphing

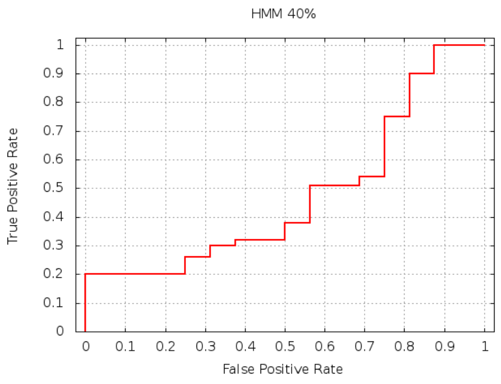

Figure A.4: ROC for HMM 40% morphing

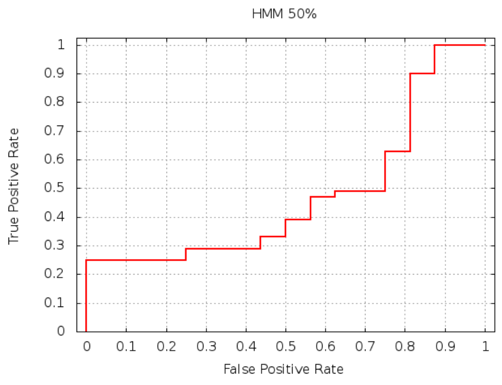

Figure A.5: ROC for HMM 50% morphing

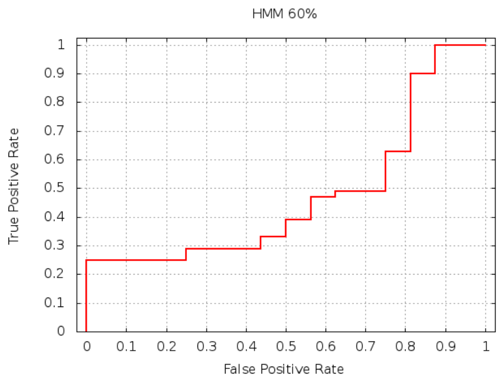

Figure A.6: ROC for HMM 60% morphing

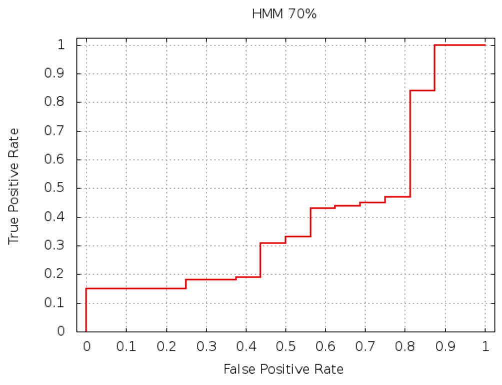

Figure A.7: ROC for HMM 70% morphing

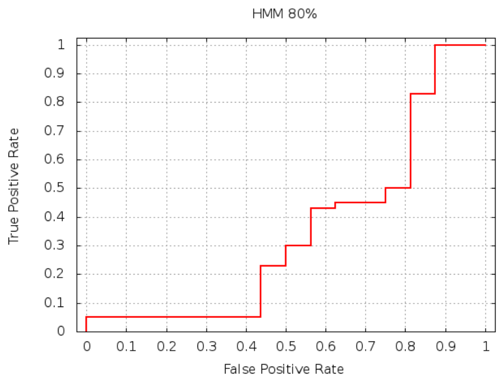

Figure A.8: ROC for HMM 80% morphing

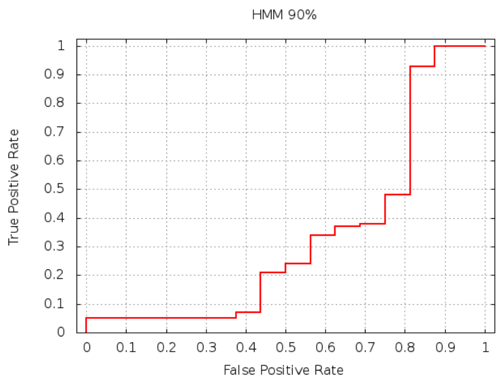

Figure A.9: ROC for HMM 90% morphing

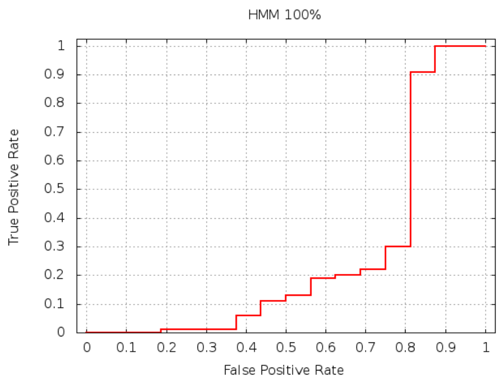

Figure A.10: ROC for HMM 100% morphing

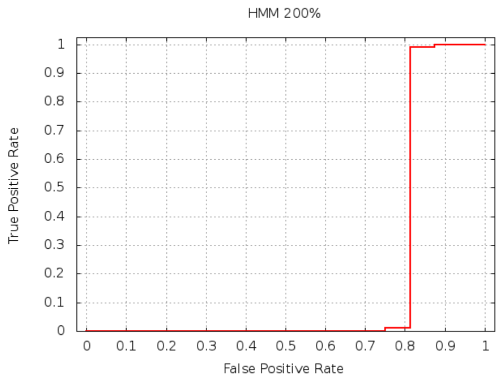

Figure A.11: ROC for HMM 200% morphing

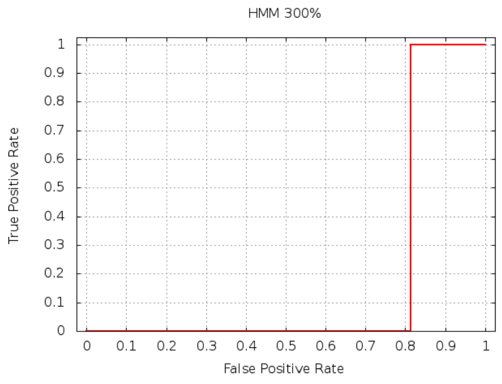

Figure A.12: ROC for HMM 300% morphing

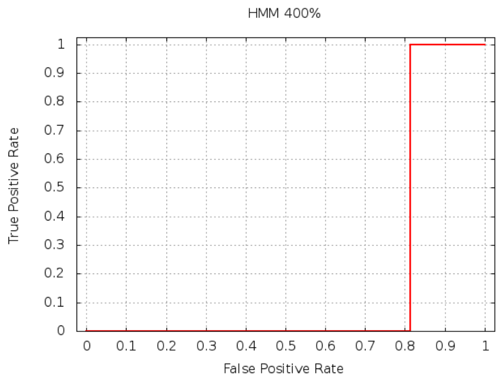

Figure A.13: ROC for HMM 400% morphing

A.2 ROC Curve for Opcode Graph Similarity

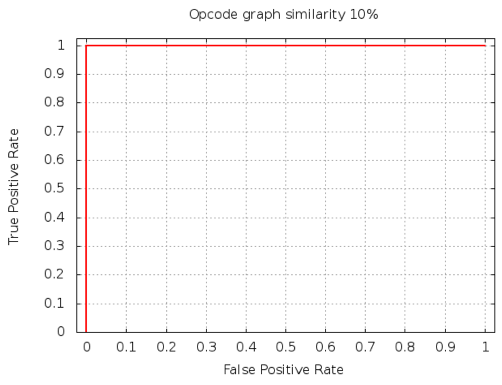

Figure A.14: ROC for OGS 10% morphing

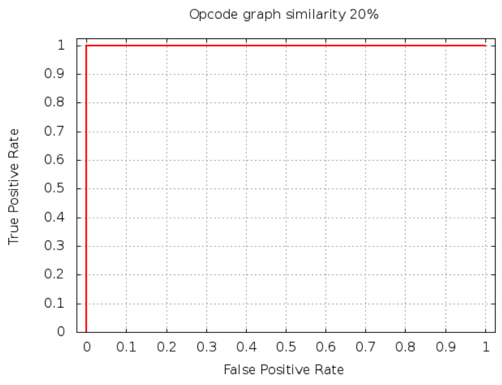

Figure A.15: ROC for OGS 20% morphing

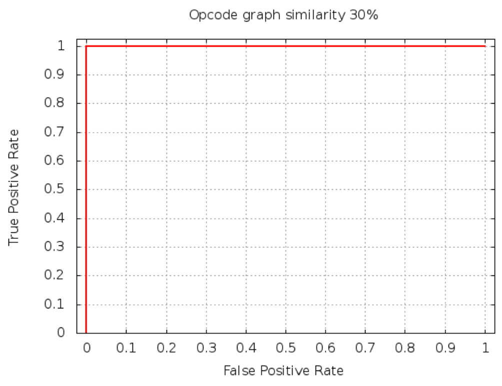

Figure A.16: ROC for OGS 30% morphing

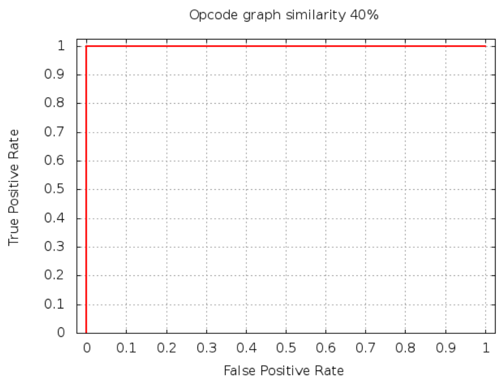

Figure A.17: ROC for OGS 40% morphing

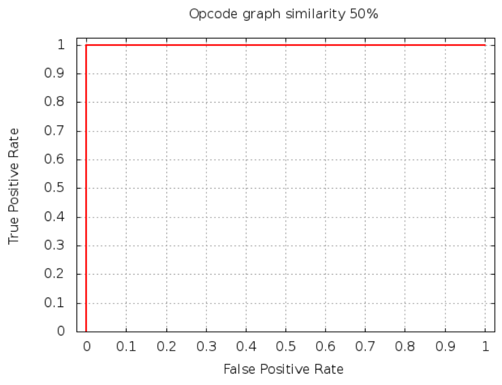

Figure A.18: ROC for OGS 50% morphing

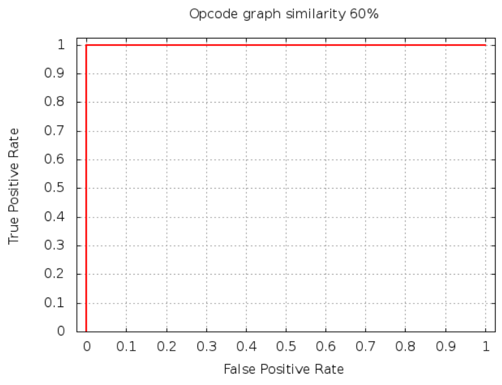

Figure A.19: ROC for OGS 60% morphing

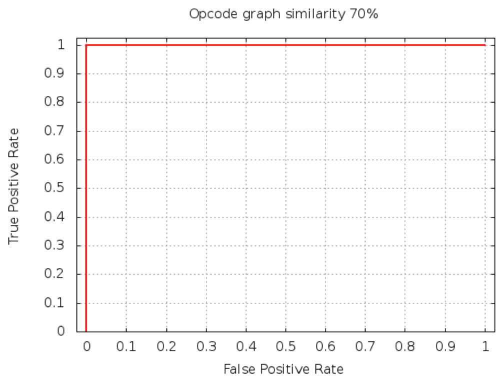

Figure A.20: ROC for OGS 70% morphing

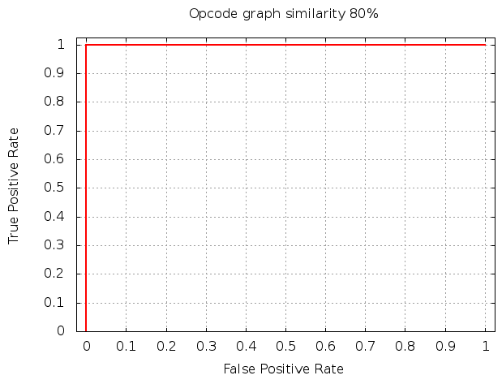

Figure A.21: ROC for OGS 80% morphing

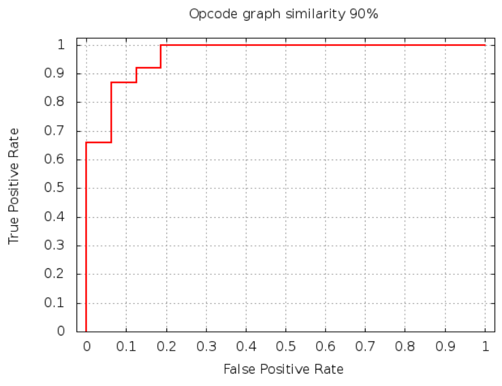

Figure A.22: ROC for OGS 90% morphing

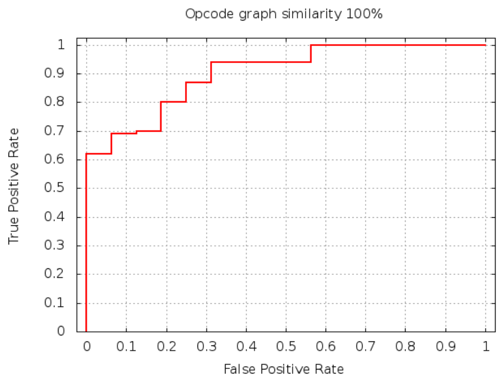

Figure A.23: ROC for OGS 100% morphing

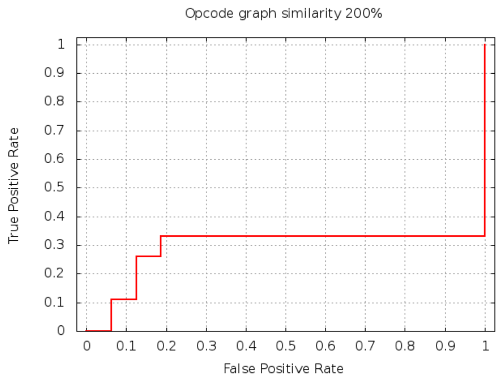

Figure A.24: ROC for OGS 200% morphing

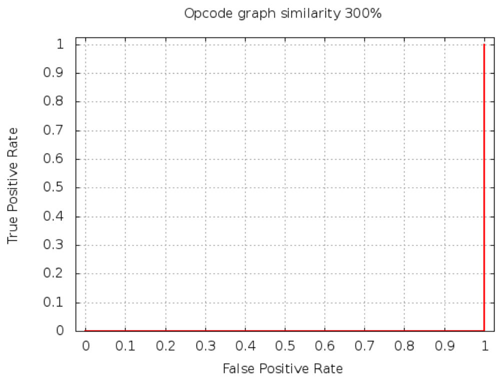

Figure A.25: ROC for OGS 300% morphing

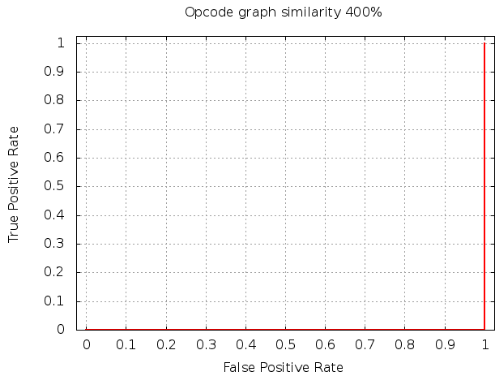

Figure A.26: ROC for OGS 400% morphing

A.3 ROC Curve for Simple Substitution Distance

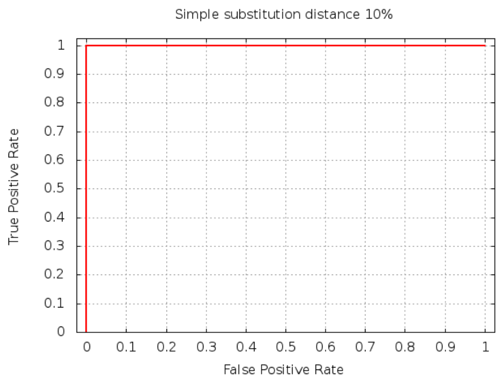

Figure A.27: ROC for SS 10% morphing

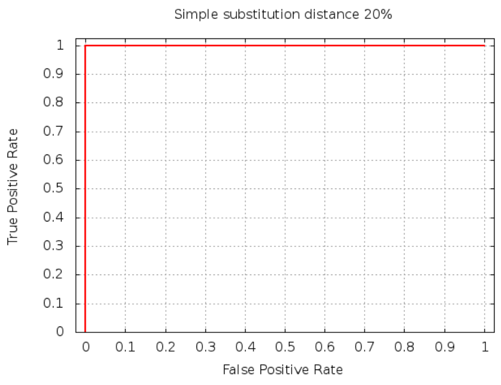

Figure A.28: ROC for SS 20% morphing

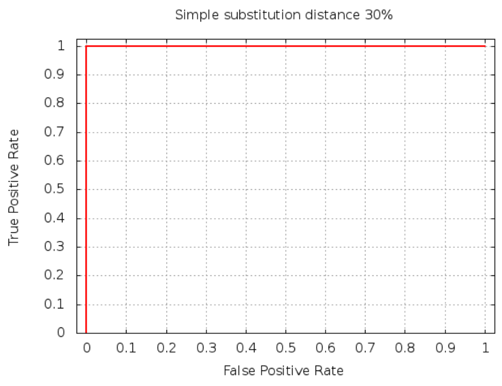

Figure A.29: ROC for SS 30% morphing

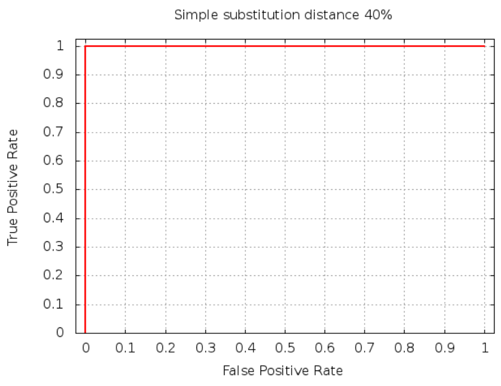

Figure A.30: ROC for SS 40% morphing

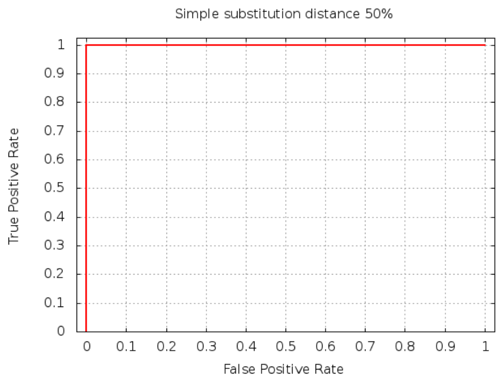

Figure A.31: ROC for SS 50% morphing

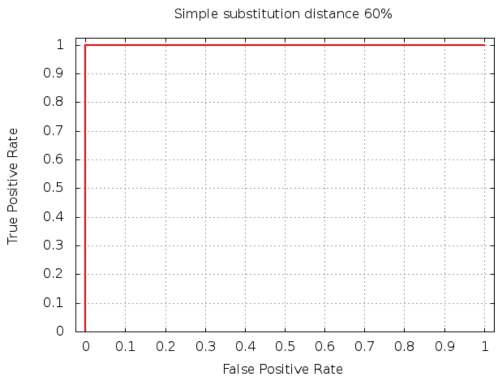

Figure A.32: ROC for SS 60% morphing

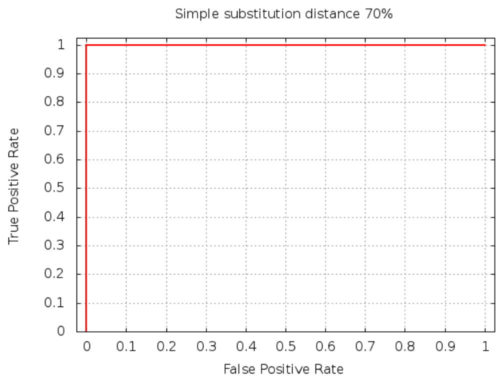

Figure A.33: ROC for SS 70% morphing

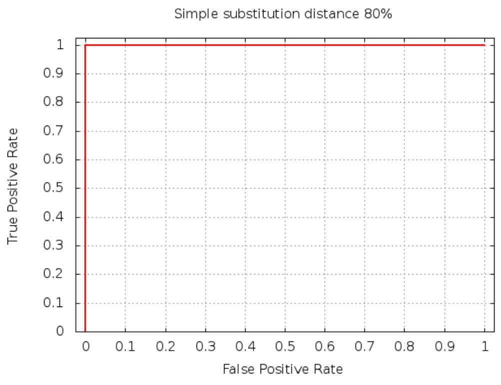

Figure A.34: ROC for SS 80% morphing

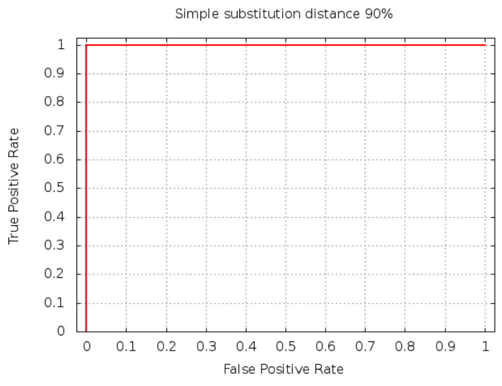

Figure A.35: ROC for SS 90% morphing

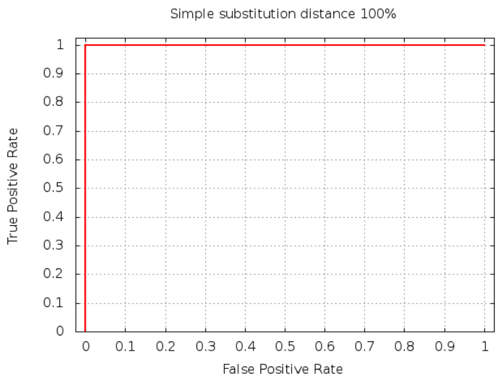

Figure A.36: ROC for SS 100% morphing

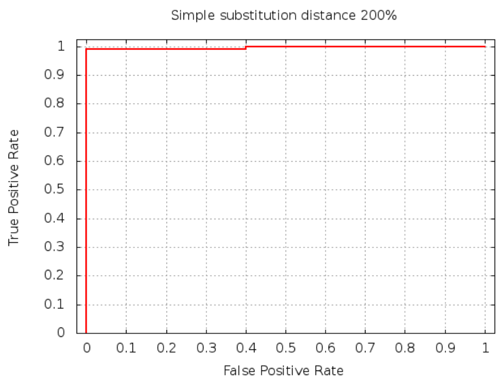

Figure A.37: ROC for SS 200% morphing

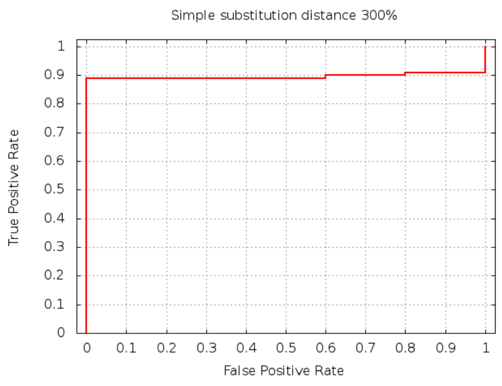

Figure A.38: ROC for SS 300% morphing

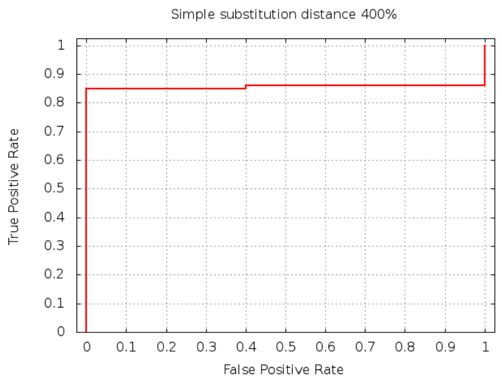

Figure A.39: ROC for SS 400% morphing

A.4 ROC Curve for Singular Value Decomposition

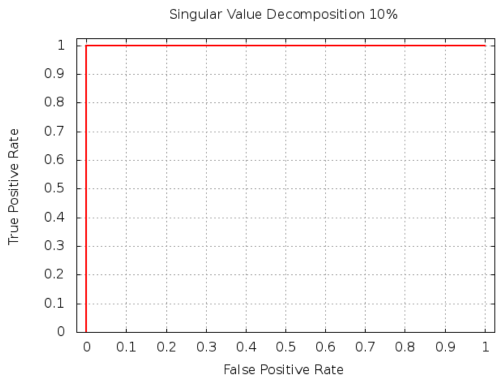

Figure A.40: ROC for SVD 10% morphing

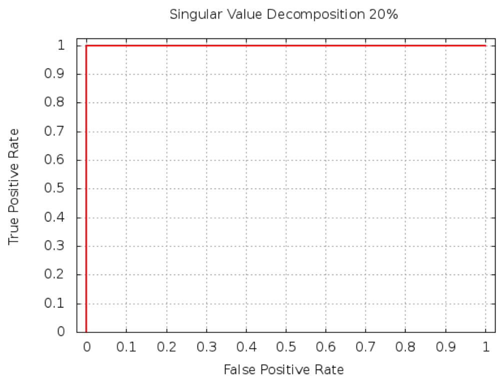

Figure A.41: ROC for SVD 20% morphing

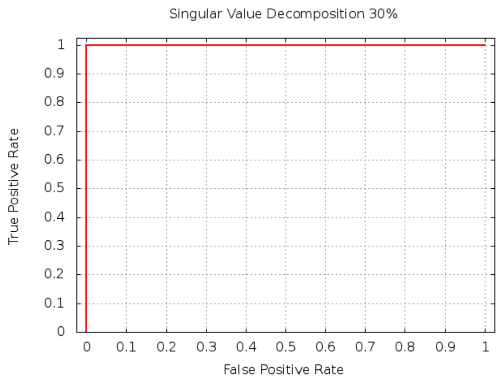

Figure A.42: ROC for SVD 30% morphing

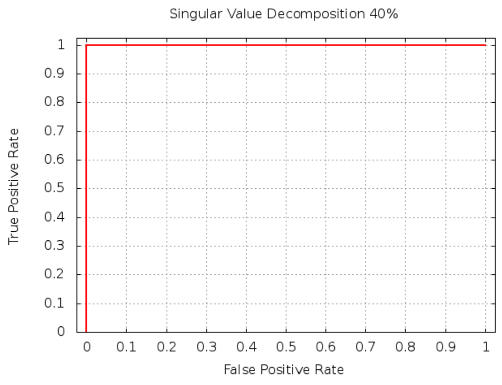

Figure A.43: ROC for SVD 40% morphing

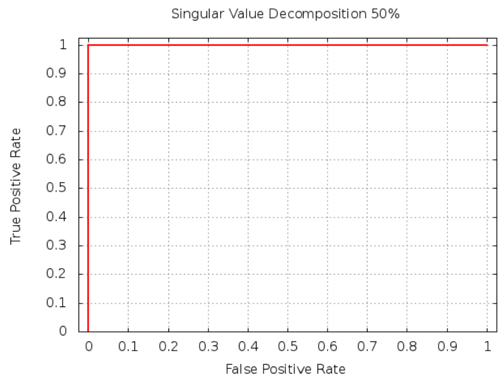

Figure A.44: ROC for SVD 50% morphing

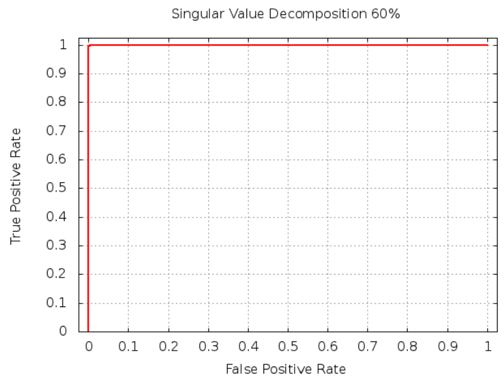

Figure A.45: ROC for SVD 60% morphing

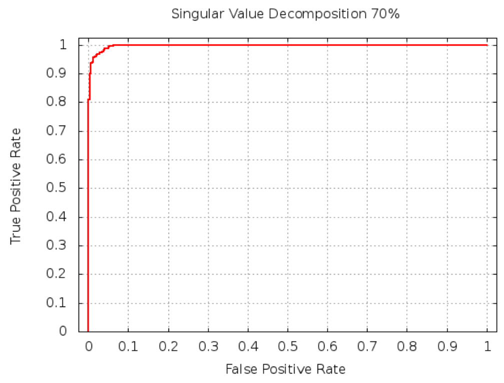

Figure A.46: ROC for SVD 70% morphing

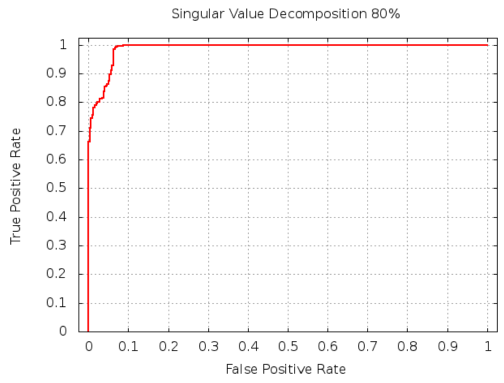

Figure A.47: ROC for SVD 80% morphing

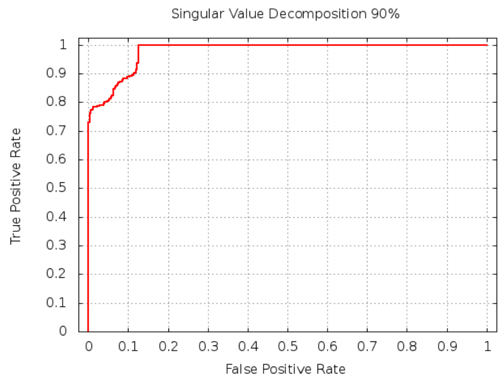

Figure A.48: ROC for SVD 90% morphing

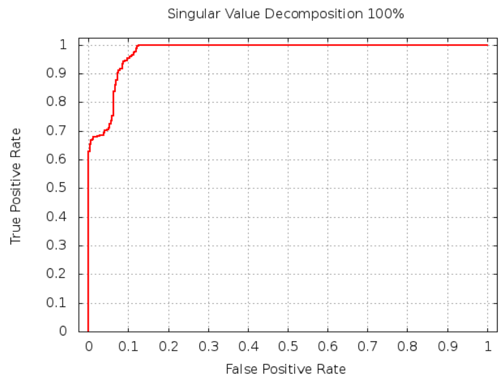

Figure A.49: ROC for SVD 100% morphing

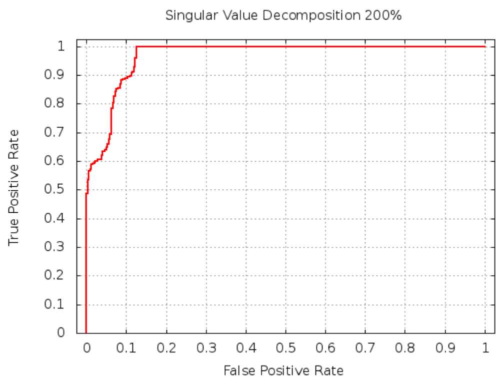

Figure A.50: ROC for SVD 200% morphing

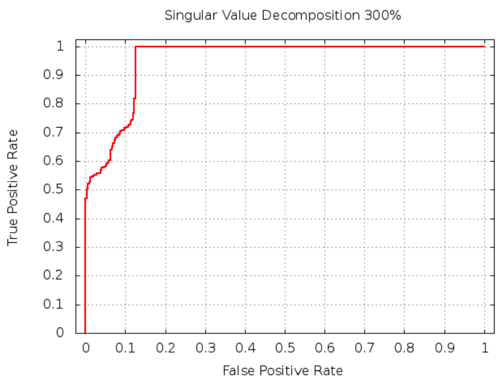

Figure A.51: ROC for SVD 300% morphing

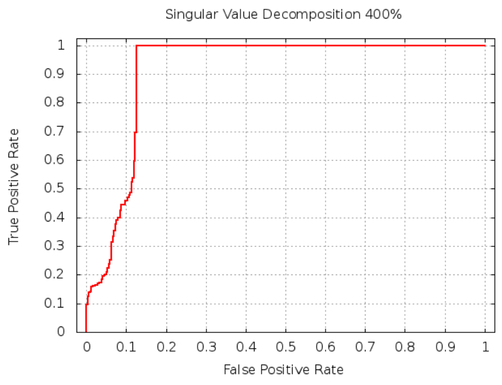

Figure A.52: ROC for SVD 400% morphing

A.5 ROC Curv for Compression-Based Analysis

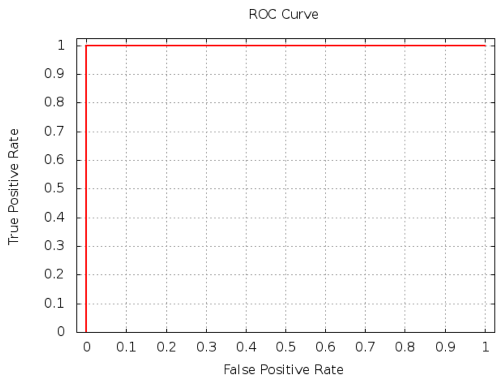

Figure A.53: ROC for for CBA 10% morphing

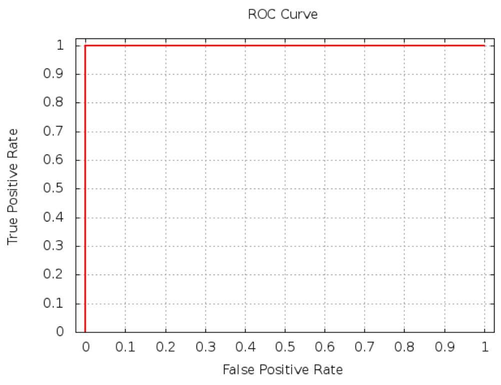

Figure A.54: ROC for for CBA 20% morphing

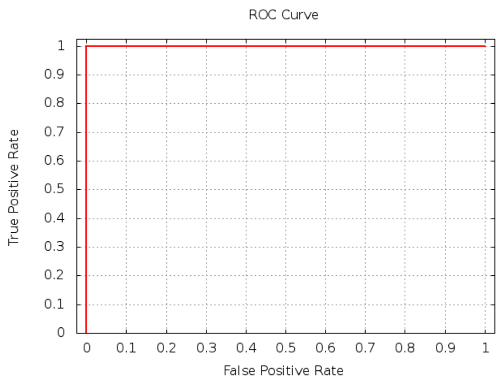

Figure A.55: ROC for for CBA 30% morphing

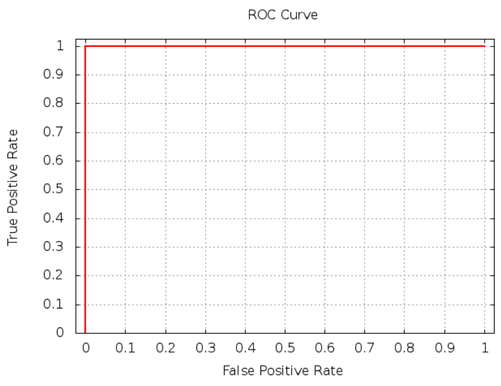

Figure A.56: ROC for for CBA 40% morphing

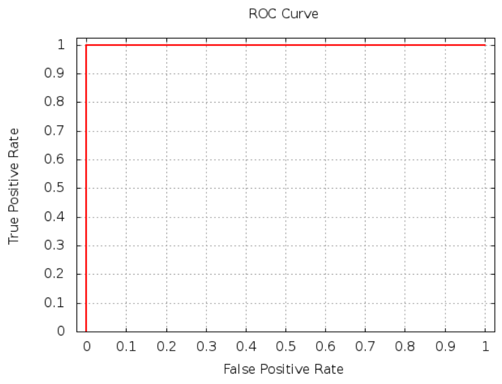

Figure A.57: ROC for for CBA 50% morphing

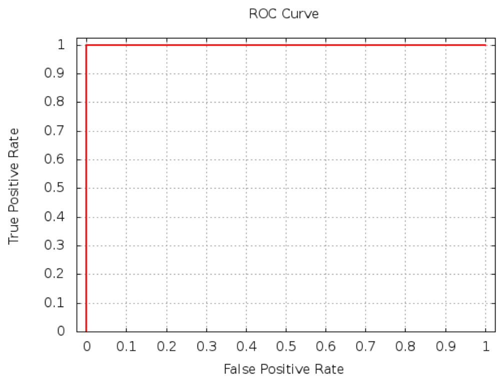

Figure A.58: ROC for for CBA 60% morphing

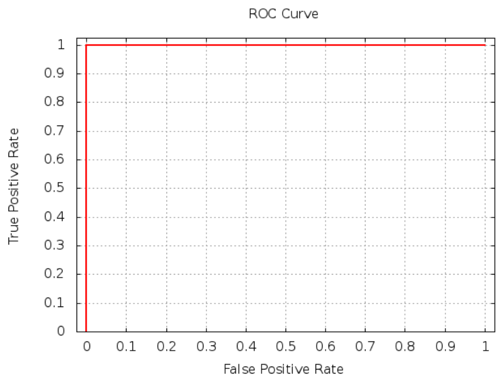

Figure A.59: ROC for for CBA 70% morphing

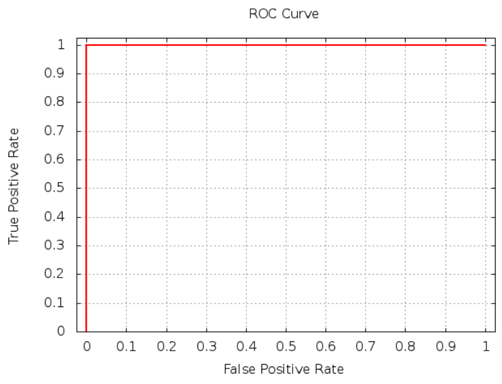

Figure A.60: ROC for for CBA 80% morphing

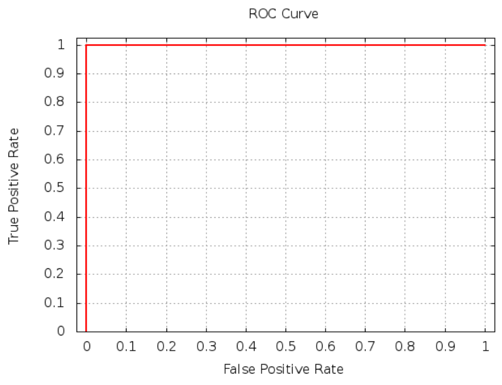

Figure A.61: ROC for for CBA 90% morphing

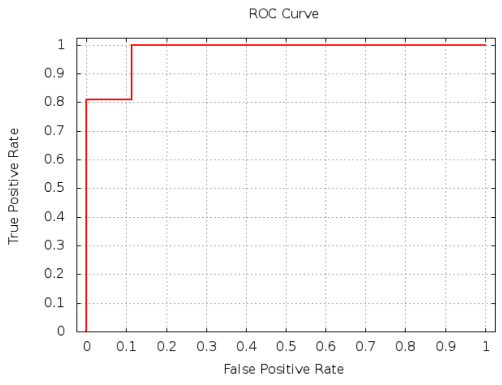

Figure A.62: ROC for for CBA 100% morphing

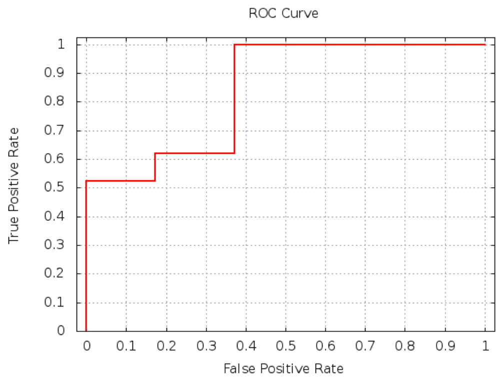

Figure A.63: ROC for for CBA 200% morphing

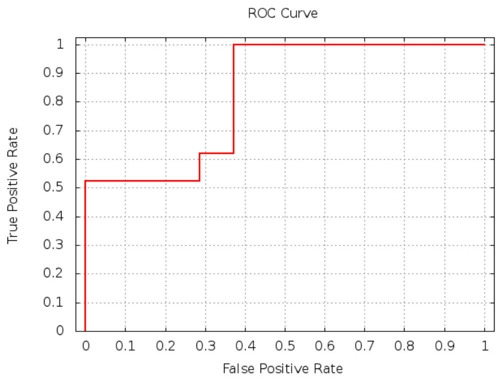

Figure A.64: ROC for for CBA 300% morphing

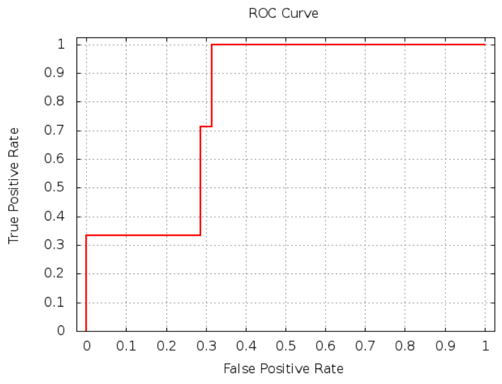

Figure A.65: ROC for for CBA 400% morphing